

Heavy Metal Azides | Hot Paper |

Binary Polyazides of Cadmium and Mercury

Axel Schulz^[a, b] and Alexander Villinger*^[a]

Abstract: Following our interest in binary element–nitrogen compounds we report here on the synthesis and comprehensive characterization (M.p., IR/Raman, elemental analysis, ¹⁴N/¹³³Cd/¹⁹⁹Hg NMR) of tri- and tetraazido cadmate and mercurate anions [E(N₃)_(2+n)]ⁿ⁻ (E = Cd, Hg; n = 1, 2) in a series of [Ph₄P]⁺ and [PNP]⁺ ([PNP]⁺ = bis(triphenylphosphine)-iminium) salts. The azide/chloride exchange in CH₂Cl₂ as well as the formation of tetrazolate salts in CH₃CN solutions of

the polyazido mercurates were investigated. Single crystal X-ray structures of all new compounds, and for comparison [Ph₄P][Cd₂(N₃)₅(H₂O)], were determined. Moreover, the synthesis of anhydrous cadmium(II) azide and its DMSO adduct is presented for the first time. For a better understanding of structure and bonding in E(N₃)₂, [E(N₃)₃]⁻ and [E(N₃)₄]²⁻, theoretical calculations at the M06-2X/aug-cc-pVDZ level were carried out.

Introduction

Like most binary transition metal–nitrogen compounds, mercury and cadmium azides represent a class of highly endothermic compounds. The difficulties in the isolation and handling of such nitrogen-rich compounds arise from their highly endothermic character, leading often to explosive decomposition.^[1] Nevertheless, as early as 1890 Curtius reported on the isolation of mercury(I) azide Hg₂(N₃)₂ by combining aqueous mercury(I) nitrate or elemental mercury with hydrazoic acid HN₃, while mercury(II) azide α-Hg(N₃)₂ was first prepared by Berthelot et al. in the year 1894 by the reaction of mercury(II) oxide and HN₃ in aqueous solution.^[2a, b]

The first vibrational characterization of both azides could be carried out by Dehnicke et al. in 1968.^[3a] Nowadays, both mercury azides are more conveniently obtained by the precipitation from aqueous solutions of mercury(I) or (II) nitrate with sodium azide. After washing and drying in air, Hg₂(N₃)₂ and α-Hg(N₃)₂ are obtained as pure, colorless microcrystalline solids in almost quantitative yields.^[3a, 4] In addition, β-Hg(N₃)₂, a second modification of mercury(II) azide, can be prepared by slow diffusion of aqueous NaN₃ solution into a solution of mercury(II) nitrate which is separated by a layer of aqueous NaNO₃.^[3c, 4c] Only recently, we reported on the successful isolation and characterization of this highly labile polymorph,

which frequently detonates spontaneously during crystal growth.^[5]

Moreover, the nitridodimercury azide [Hg₂N]N₃, the azide of Millon's base, which features a three-dimensional cationic [Hg₂N]⁺ framework structure incorporating the azide ions in the cavities, could be isolated in the reaction of α-Hg(N₃)₂ with aqueous ammonia by our group.^[2a, 5, 6]

Numerous organomercury(II) azides RHgN₃ including alkyl, aryl and perfluorinated derivatives are known and were thoroughly investigated.^[7] However, only lately Klapötke et al. observed that organomercury(II) azides easily reacted in a 1,3-dipolar cycloaddition reaction with organonitriles forming tetrazole rings.^[7g] Thereby, the reaction is regioselective and even non-activated (electron rich) nitriles such as acetonitrile could be applied. All binary mercury azides were comprehensively studied by vibrational spectroscopy (IR/Raman),^[3a, b, 5] spectrophotometric methods,^[4a] X-ray powder diffraction,^[3b, 5] single-crystal X-ray diffraction,^[4b, 5] and thermal analysis.^[3c–e, 5] On the other hand, only little is known about polyazido mercurates. While the tetraazido mercurate anion [Hg(N₃)₄]²⁻ is unknown in literature, Beck et al. described the triazido mercurate anion [Hg(N₃)₃]⁻ in the salt [Ph₄P][Hg(N₃)₃], which could be characterized by vibrational methods, however, structural data is not available.^[8]

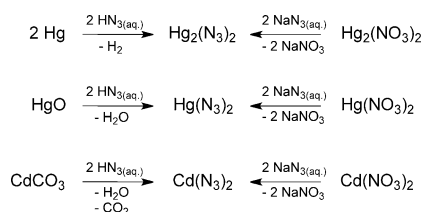
The first synthesis of cadmium(II) azide dates back to the year 1898, when Curtius and Rissom reported on the reaction of cadmium(II) carbonate and excess aqueous HN₃ affording pale yellow crystals, which were characterized as insensitive to impact (Scheme 1).^[9a] Later, Birckenbach and Wöhler et al. could demonstrate that pure colorless Cd(N₃)₂ is highly sensitive to impact and shock.^[3e, 9b] Recently, Schnick et al. succeeded in the first vibrational and structural characterization of cadmium(II) azide.^[10] While the former reaction never led to detonations during the preparation of cadmium(II) azide,^[9, 3c, 10] Bassière reported an alternative procedure starting from cadmium(II) nitrate and sodium azide, which frequently result-

[a] Prof. Dr. A. Schulz, Dr. A. Villinger
Institut für Chemie, Universität Rostock
Albert-Einstein-Strasse 3a, 18059 Rostock (Germany)
E-mail: alexander.villinger@uni-rostock.de

[b] Prof. Dr. A. Schulz
Abteilung Materialdesign
Leibniz-Institut für Katalyse e.V. an der Universität Rostock
Albert-Einstein-Strasse 29a, 18059 Rostock (Germany)

Supporting information for this article is available on the WWW under <http://dx.doi.org/10.1002/chem.201406023>.

ed in spontaneous explosions of the crystal growth solution,^[11a] later confirmed by Reckeweg and Simon.^[11b] Contrary to α - $\text{Hg}(\text{N}_3)_2$, cadmium(II) azide is hygroscopic and slowly decomposes in air forming yellow basic products. Nevertheless, an anhydrous synthesis has not been reported so far.^[9a, 11a, 10] Cadmium(II) azide reacts readily with aqueous ammonia, forming the stable complex $\text{Cd}(\text{N}_3)_2(\text{NH}_3)_2$ which shows no further condensation as compared to mercury(II) azide (vide supra).^[6] Accordingly, many adducts of cadmium(II) azide with bases such as pyridine or ethylenediamine were prepared and structurally characterized.^[9a, 6, 12] In 1967, Beck et al. reported on the synthesis of the first polyazido cadmate in the salt $[\text{Ph}_4\text{P}][\text{Cd}_2(\text{N}_3)_5(\text{H}_2\text{O})]$.^[8] Since no single-crystal X-ray data is available, the constitution of the formal pentaazido dicadmiate(II) anion $[\text{Cd}_2(\text{N}_3)_5]^-$ remains unknown. The first evidence for a triazido cadmate anion was found by Clegg and Krischner in the structure of $\text{K}[\text{Cd}(\text{N}_3)_3]\cdot\text{H}_2\text{O}$.^[13a] However, the former compound shows several significant short potassium azide contacts and therefore should rather be considered as K/Cd double salt. In contrast, the $[\text{Cd}(\text{N}_3)_3]^-$ anion in the salt $[\text{Me}_4\text{N}][\text{Cd}(\text{N}_3)_3]$ prepared by Mautner et al., forms a three-dimensional “perovskite-like” network consisting of $\text{Cd}(\text{N}_3)_6$ octahedra, which are connected by $\mu_{1,3}$ -bridging azide units, while the $[\text{Me}_4\text{N}]^+$ cations reside in the large cages and are only weakly bound by van der Waals interactions.^[14] The only report for a tetraazido cadmate anion can be found in the work of Krischner et al., who described the synthesis of $\text{M}_2[\text{Cd}(\text{N}_3)_4]$ ($\text{M}=\text{K}, \text{Tl}$) from aqueous solutions of cadmium carbonate, HN_3 and KN_3 or TlN_3 , respectively.^[13b] While $\text{Tl}_2[\text{Cd}(\text{N}_3)_4]$ detonates on impact, the potassium salt is almost insensitive. Interestingly, a slight excess of TlN_3 in the reaction led to the isolation of the formal $\text{Tl}_8[\text{Cd}_3(\text{N}_3)_{14}]$ salt ($=\text{Tl}_2[\text{Cd}(\text{N}_3)_4]\cdot 6\text{Cd}(\text{N}_3)_2\cdot 6\text{TlN}_3$).^[15] Both thallium salts could be structurally characterized and also show octahedrally coordinated cadmium(II) cations, surrounded by six azide ligands.^[13a] However, besides these structure determinations and thermal analyses, the polyazido cadmates have scarcely been characterized, and vibrational data is completely missing.



Scheme 1. Different synthetic routes to $\text{Hg}_2(\text{N}_3)_2$, $\text{Hg}(\text{N}_3)_2$ and $\text{Cd}(\text{N}_3)_2$.

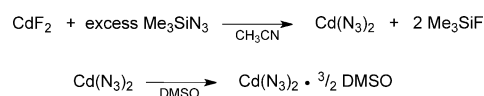
Results and Discussion

Synthesis of $\text{Cd}(\text{N}_3)_2$ and $\text{Cd}(\text{N}_3)_2\cdot\frac{3}{2}\text{DMSO}$

To avoid the presence of water during the synthesis, we decided to prepare cadmium(II) azide by means of a fluoride/azide exchange reaction in cadmium(II) fluoride (Scheme 2). The reaction of excess trimethylsilyl azide Me_3SiN_3 with freshly prepared CdF_2 in CH_3CN proceeded within one day at

ambient temperature under exclusion of light. The complete consumption of cadmium fluoride during reaction could easily be monitored by powder X-ray diffraction.^[16]

After centrifugation, washing and drying at 60–80 °C in vacuo, pure $\text{Cd}(\text{N}_3)_2$ was obtained as colorless microcrystalline solid in good yields.

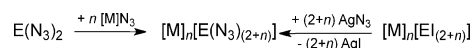


Scheme 2. Synthetic routes to $\text{Cd}(\text{N}_3)_2$ and $\text{Cd}(\text{N}_3)_2\cdot\frac{3}{2}\text{DMSO}$.

Crystalline $\text{Cd}(\text{N}_3)_2$ is shock- and friction-sensitive and explodes violently on fast heating emitting a bright blue flashlight. Cadmium(II) azide synthesized by this procedure is stable for at least two years without noticeable decomposition if stored under argon in the absence of light. Similar to α - $\text{Hg}(\text{N}_3)_2$, $\text{Cd}(\text{N}_3)_2$ can be recrystallized from acetonitrile or water, however, contrary to mercury(II) azide, which also can be obtained solvent-free from DMSO, cadmium(II) azide crystallizes as colorless DMSO solvate with the formal composition $\text{Cd}(\text{N}_3)_2\cdot\frac{3}{2}\text{DMSO}$ (Scheme 2, Figure 1). Differently to $\text{Cd}(\text{N}_3)_2$, the DMSO solvate is not sensitive to friction or shock and is even reasonably stable at 120 °C in the molten state (vide infra).^[16]

Synthesis of $[\text{M}]_n[\text{E}(\text{N}_3)_{(2+n)}]$

As illustrated in Scheme 3, two synthetic routes seemed to be feasible for preparing salts of polyazido cadmate and mercurate anions $[\text{M}]_n[\text{E}(\text{N}_3)_{(2+n)}]$ ($[\text{M}]^+$ = weakly coordinating cation = $[\text{Ph}_4\text{P}]^+$, $[\text{PNP}]^+ = [(\text{Ph}_3\text{P})_2\text{N}]^+$; $\text{E}=\text{Cd}, \text{Hg}$, with $n=1, 2$): 1) direct reaction of binary cadmium or mercury azide $\text{E}(\text{N}_3)_2$ with the corresponding phosphonium azide $[\text{M}]\text{N}_3$ in the required stoichiometry; 2) iodide/azide exchange in the tri- and tetraiodo cadmates or mercurates $[\text{M}]_n[\text{E}(\text{I})_{(2+n)}]$ by treatment with silver azide AgN_3 . In the latter reaction, it is also possible to generate the tetraiodo metallate anion $[\text{E}(\text{I})_4]^{2-}$ in situ by reaction of triiodo metallate $[\text{M}][\text{E}(\text{I})_3]$ salts with the corresponding iodide salts $[\text{M}]\text{I}$.



Scheme 3. Different synthetic routes to $[\text{E}(\text{N}_3)_{(2+n)}]^{n-}$ salts ($\text{E}=\text{Cd}, \text{Hg}$; $n=1, 2$; $[\text{M}]^+ = [\text{Ph}_4\text{P}]^+, [\text{PNP}]^+$).

While the procedure starting from binary azides avoids by-products, which facilitates the isolation of polyazido metallate salts, the manipulation with $\text{Cd}(\text{N}_3)_2$ and $\text{Hg}(\text{N}_3)_2$ always bears the risk of serious explosions. On the other hand, in the reaction of iodometallate salts with silver azide, large amounts of silver iodide precipitate have to be filtered off. However, the iodide/azide exchange reaction limits the hazards to the known risks during handling neat AgN_3 . The required polyiodo

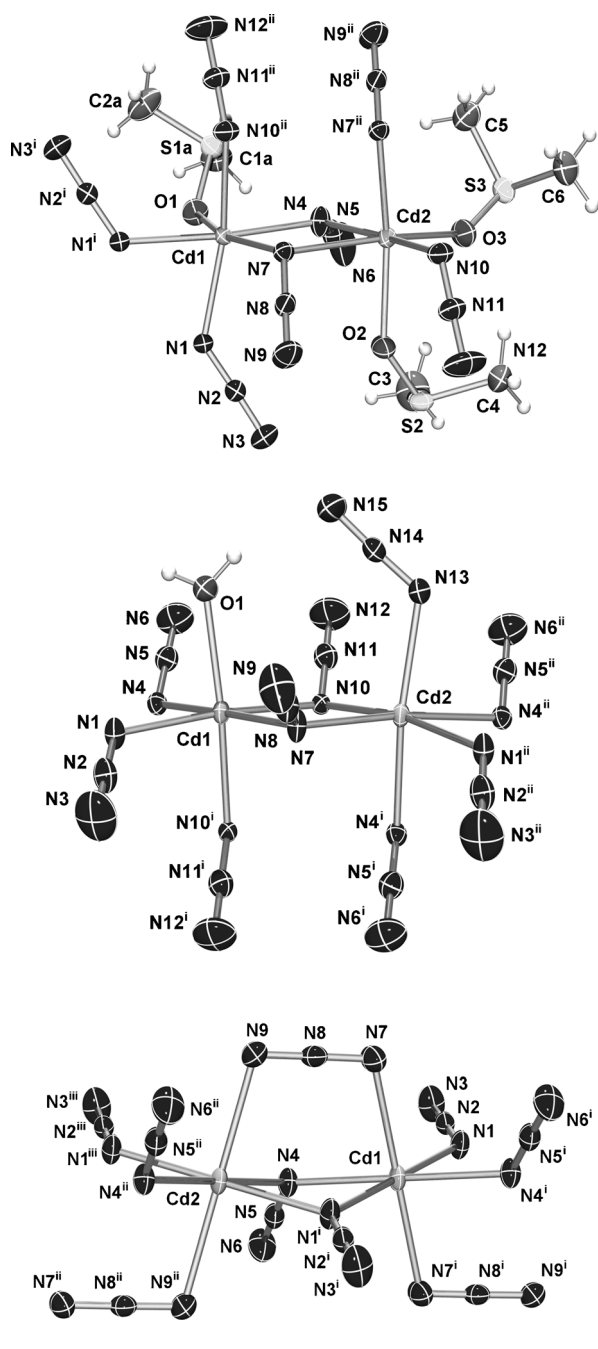


Figure 1. ORTEP drawings of the coordination sphere of Cd(N₃)₂·³/₂ DMSO (top), [Ph₄P][Cd₂(N₃)₅(H₂O)] (middle) and [Ph₄P][Cd(N₃)₃] (bottom) in the crystal. Thermal ellipsoids with 50% probability at 173 K. Disorder not displayed. Selected bond lengths [Å]: Cd(N₃)₂·³/₂ DMSO (symmetry codes: (i) $-x+2, -y+1, -z$; (ii) $-x+1, -y+1, -z$): Cd1–N1 2.273(1), Cd1–O1 2.316(1), Cd1–N4 2.321(1), Cd1–N1ⁱ 2.322(1), Cd1–N10ⁱ 2.329(1), Cd1–N7 2.431(1), Cd2–O2 2.249(1), Cd2–N4 2.273(1), Cd2–O3 2.282(1), Cd2–N10 2.283(1), Cd2–N7ⁱⁱ 2.348(1), Cd2–N7 2.513(1), N1–N2 1.207(2), N2–N3 1.141(2), N4–N5 1.196(2), N5–N6 1.141(2), N7–N8 1.217(2), N8–N9 1.141(2), N10–N11 1.196(2), N11–N12 1.153(2); [Ph₄P][Cd₂(N₃)₅(H₂O)] (symmetry codes: (i) $-x+2, -y+1, -z+1$; (ii) $x+1, y, z$): Cd1–N1 2.267(2), Cd1–N7 2.284(2), Cd1–O1 2.302(2), Cd1–N10 2.338(2), Cd1–N4 2.381(2), Cd1–N10ⁱ 2.415(2), Cd2–N13 2.285(2), Cd2–N1ⁱⁱ 2.308(2), Cd2–N7 2.310(2), Cd2–N4ⁱ 2.351(2), Cd2–N4ⁱⁱ 2.410(2), Cd2–N10 2.416(2), N1–N2 1.193(3), N2–N3 1.140(3), N4–N5 1.230(3), N5–N6 1.145(3), N7–N8 1.193(3), N8–N9 1.149(3), N10–N11 1.220(3), N11–N12 1.135(3), N13–N14 1.182(3), N14–N15 1.154(3); [Ph₄P][Cd(N₃)₃] (symmetry codes: (i) $-x+2, -y, -z+1$; (ii) $-x+1, -y, -z+1$; (iii) $x-1, y, z$): Cd1–N4 2.316(2), Cd1–N4ⁱ 2.316(2), Cd1–N7ⁱ 2.357(2), Cd1–N7 2.357(2), Cd1–N1 2.4078(2), Cd1–N1ⁱ 2.408(2), Cd2–N4 2.332(2), Cd2–N4ⁱⁱ 2.332(2), Cd2–N1ⁱⁱⁱ 2.347(2), Cd2–N1ⁱ 2.347(2), Cd2–N9ⁱⁱ 2.397(2), Cd2–N9 2.397(2), N6–N5 1.150(2), N3–N2 1.147(2), N1–N2 1.203(2), N4–N5 1.205(2), N9–N8 1.177(2), N8–N7 1.179(2).

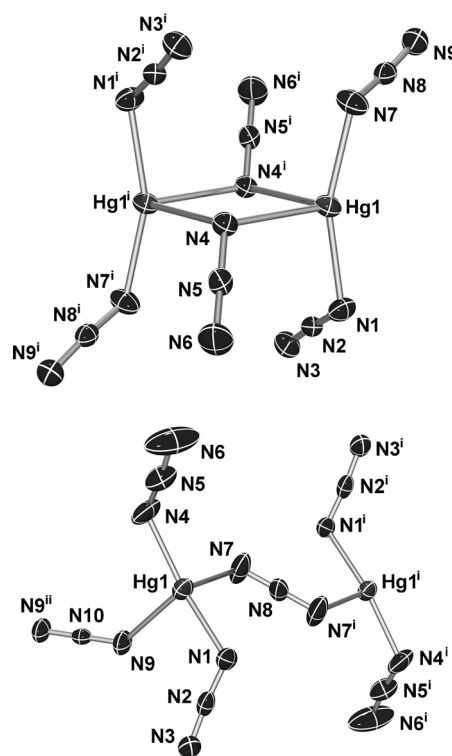


Figure 2. ORTEP drawings of the coordination spheres of the anions in [Ph₄P][Hg(N₃)₃] (top) and [PNP][Hg(N₃)₃] (bottom) in the crystal. Thermal ellipsoids with 50% probability at 173 K. Selected bond lengths [Å]: [Ph₄P][Hg(N₃)₃] (symmetry code: (i) $-x+2, -y+1, -z+1$; (ii) $-x+1, -y+1, -z+1$): Hg1–N1 2.113(2), Hg1–N7 2.097(2), Hg1–N4 2.452(2), Hg1–N4ⁱ 2.570(1), Hg1–N1ⁱⁱ 2.966(2), N1–N2 1.213(2), N2–N3 1.143(2), N4–N5 1.199(2), N4–Hg1 2.574(2), N5–N6 1.154(2), N7–N8 1.202(2), N8–N9 1.146(2); [PNP][Hg(N₃)₃] (symmetry code: (i) $-x, -y+1, -z$): Hg1–N4 2.077(4), Hg1–N1 2.089(3), Hg1–N9 2.467(3), Hg1–N7 2.485(4), N1–N2 1.202(5), N2–N3 1.145(5), N4–N5 1.187(5), N5–N6 1.121(5), N7–N8 1.165(4), N8–N7ⁱ 1.165(4), N9–N10 1.170(3), N10–N9ⁱ 1.170(3).

metallate salts can easily be prepared by the reaction of cadmium(II)- or mercury(II) iodide with the corresponding phosphonium iodide [M]I in acetone or dichloromethane, respectively. After heating to reflux, precipitation and washing with *n*-pentane and drying in vacuo, all polyiodo cadmate and mercurate salts are obtained as colorless, microcrystalline solids in almost quantitative yields.^[16b]

We found, that in the present study, both synthetic routes according to Scheme 3 gave almost identical results. However, while salts of triazido- and tetraazido mercurate anions with both different phosphonium cations could successfully be isolated, not all possible combinations of polyazido cadmate anion and cation were found to be stable in the solid state

(Figures 1–3). Both azido cadmates [Ph₄P][Cd(N₃)₃] and [PNP]₂[Cd(N₃)₄] were easily prepared as colorless microcrystalline solids from [Ph₄P][CdI₃] or [PNP][CdI₃]/[PNP]I, respectively, with AgN₃. Likewise, the reactions of Cd(N₃)₂ with stoichio-

metric amounts of $[M]N_3$ in polar solvents such as acetonitrile or DMSO proceeded in good yields.

In contrast, it was impossible to isolate the formal triazido cadmate $[Cd(N_3)_3]^-$ bearing the bulky $[PNP]^+$ cation, as well as the tetraazido cadmate $[Cd(N_3)_4]^{2-}$ with the smaller $[Ph_4P]^+$ cation ($V_{ion}: [Ph_4P]^+ 464$ vs. $[PNP]^+ 723 \text{ \AA}^3$),^[17] since these solutions always deposited crystals of the corresponding tetra- or triazido cadmate salts, respectively, almost independently of the stoichiometry. During many crystallization attempts, only traces of $[Ph_4P]_2[Cd(N_3)_4]$ could be identified by single crystal X-ray diffraction, however, without any further analytical characterization.^[16] Interestingly, besides these tri- and tetraazido cadmates, the formation of a pentaazido dicadmite anion as reported in the salt $[Ph_4P][Cd_2(N_3)_5(H_2O)]$ was not observed. Therefore, we prepared the latter compound in analogy to the procedure given in literature from the reaction of $[Ph_4P]Cl$, NaN_3 and cadmium(II) sulfate in water.^[6] While all analytical data compare very well to those reported by Beck et al., we found that in contrast to the conclusions of the authors, $[Ph_4P][Cd_2(N_3)_5(H_2O)]$ could be recrystallized from hot water without decomposition, in good yields. However, if the pentaazido dicadmite salt was recrystallized from CH_3CN , only the triazido cadmate salt $[Ph_4P][Cd(N_3)_3]$ instead of a possible acetonitrile adduct was obtained.

Contrary to the polyazido cadmates, tri- and tetraazido mercurates $[PNP][Hg(N_3)_3]$ and $[PNP]_2[Hg(N_3)_4]$ from the reaction of $Hg(N_3)_2$ with $[PNP]N_3$ in acetonitrile, as well as both $[Ph_4P]^+$ mercurate salts, obtained from $[Ph_4P][HgI_3]$ and AgN_3 or $Hg(N_3)_2$ and $[Ph_4P]N_3$ in acetonitrile or DMSO could be successfully isolated as colorless crystalline solids. In case of the $[Ph_4P]^+$ salts, however, a pronounced influence of solvent polarity on the crystallization was observed. While solutions of acetonitrile and dichloromethane promote the deposition of $[Ph_4P][Hg(N_3)_3]$ almost independently of the stoichiometry, crystalline tetraazido mercurate $[Ph_4P]_2[Hg(N_3)_4]$ was only accessible from polar, very concentrated DMSO solutions. It is interesting to note, that the reaction of mercury(II) azide with $[Ph_4P]N_3$ could also be applied in the preparation of $[Ph_4P]_2[Hg(N_3)_4]$, since $Hg_2(N_3)_2$ readily disproportionates into $Hg(N_3)_2$ and elemental mercury in acetonitrile. It is worthwhile to mention, that all analytical data of $[Ph_4P][Hg(N_3)_3]$ (M.p., IR/Raman) are in good agreement with the values found in literature.^[8]

Furthermore, we investigated the stability of tetraphenylphosphonium polyazido mercurates in dichloromethane solutions with regard to a Cl^-/N_3^- exchange.^[16,18] When a highly concentrated solution of $[Ph_4P]_2[Hg(N_3)_4]$ was stored at ambient temperature for one week, depending on the reaction and crystallization time, species such as $[Ph_4P][Hg(N_3)_{1.84}Cl_{1.16}]$ and $[Ph_4P]_2[Hg(N_3)_{1.42}Cl_{2.58}]$, which display a partial substitution of the azide groups by chloride atoms, could be isolated and characterized by single crystal X-ray analyses. For $[Ph_4P][Hg(N_3)_{1.84}Cl_{1.16}]$, a melting point of $139^\circ C$ was determined, which is only slightly lower compared to pure triazido mercurate ($[Ph_4P][Hg(N_3)_3]$, $147^\circ C$). Contrarily, for $[Ph_4P][Hg(N_3)_3]$ a considerably slower exchange rate was observed indicating a larger complex stabilization constant. Nevertheless, when the synthesis of $[Ph_4P][Hg(N_3)_3]$ was performed in dichloromethane

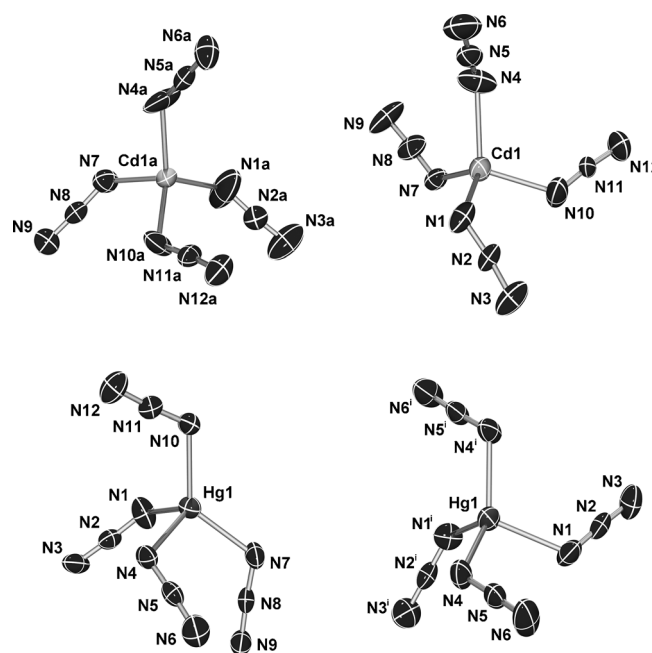


Figure 3. ORTEP drawings of the molecular structure of the $[E(N_3)_3]^{2-}$ anions in the crystal (left: $[Ph_4P]^+$, right: $[PNP]^+$ salt). Thermal ellipsoids with 50% probability at 173 K. Disorder not displayed. Selected bond lengths [\AA]: $[Ph_4P][Cd(N_3)_3]$: Cd1a–N4a 2.160(4), Cd1a–N7 2.185(3), Cd1a–N10a 2.197(7), Cd1a–N1a 2.224(5), N1a–N2a 1.179(9), N2a–N3a 1.110(8), N4a–N5a 1.183(4), N5a–N6a 1.147(8), N7–N8 1.191(3), N8–N9 1.151(3), N10a–N11a 1.183(4), N11a–N12a 1.147(8); $[PNP][Cd(N_3)_3]$: Cd1–N7 2.08(2), Cd1–N10 2.194(4), Cd1–N4 2.205(5), Cd1–N1 2.29(2), N1–N2 1.195(7), N2–N3 1.160(7), N4–N5 1.159(8), N5–N6 1.137(9), N7–N8 1.191(7), N8–N9 1.160(7), N10–N11 1.156(8), N11–N12 1.130(8); $[Ph_4P][Hg(N_3)_3]$: Hg1–N10 2.184(2), Hg1–N7 2.189(2), Hg1–N4 2.294(2), Hg1–N1 2.295(2), N1–N2 1.183(2), N2–N3 1.155(2), N4–N5 1.203(2), N5–N6 1.152(2), N7–N8 1.197(2), N8–N9 1.153(2), N10–N11 1.202(2), N11–N12 1.151(2); $[PNP][Hg(N_3)_3]$ (symmetry code: (i) $-x+1, y, -z+3/2$): Hg1–N4 2.180(2), Hg1–N4ⁱ 2.180(2), Hg1–N1ⁱ 2.286(2), Hg1–N1 2.286(2), N1–N2 1.183(3), N2–N3 1.160(3), N4–N5 1.190(2), N5–N6 1.143(3).

as solvent, the crystalline product was also found to be slightly contaminated by chloride ($[Ph_4P][Hg(N_3)_{2.94}Cl_{0.06}]$) as deduced from a single X-ray structure determination (Figure 4).^[16] Interestingly, vibrational spectroscopy (IR/Raman) and melting-point determination are not completely suited to detect such small chloride impurities. Only recently, the stability of $[Ph_4P]N_3$ and $[Ph_4P]_3[Bi(N_3)_6]$ in chlorinated solvents was investigated by our group, which displayed a reversible reaction for the Cl^-/N_3^- exchange, following a second order rate law.^[18c] In any case, to exclude a possible chloride/azide exchange, DMSO and CH_3CN should be used as solvents for chloride-free synthesis of polyazido metallate salts.

Moreover, we observed the formation of methyltetrazolate salts as an interesting side reaction in concentrated acetonitrile solutions of polyazido mercurates bearing the bulky $[PNP]^+$ cation. The diazido methyltetrazolato mercurate salt $[PNP][Hg(N_3)_2(CH_3CN_4)]$ as CH_3CN hemisolvate was isolated in small amounts as colorless needle-like crystals from concentrated CH_3CN solutions of $[PNP]_2[Hg(N_3)_4]$ after storage for several days at $5^\circ C$ (Scheme 4). The tetrazolate salt could be recrystallized from DMSO to give the solvent free compound. Both

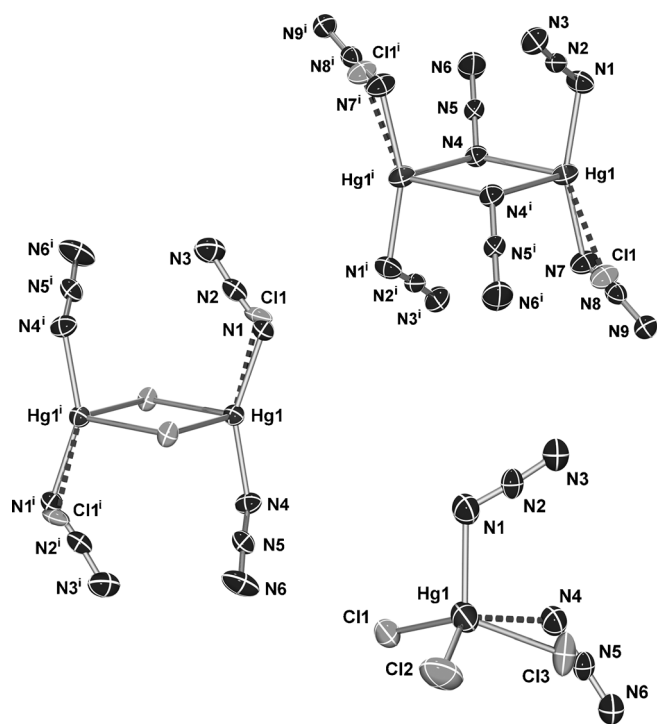
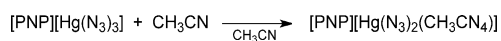


Figure 4. ORTEP drawings of the molecular structure of the anions $[\text{Hg}(\text{N}_3)_{2.94}\text{Cl}_{0.06}]^-$ (top), $[\text{Hg}(\text{N}_3)_{1.84}\text{Cl}_{1.16}]^-$ (middle) and $[\text{Hg}(\text{N}_3)_{1.42}\text{Cl}_{2.58}]^{2-}$ (bottom) in the crystal. Thermal ellipsoids with 50% probability at 173 K. Selected bond lengths [Å]: $[\text{Ph}_4\text{P}][\text{Hg}(\text{N}_3)_{2.94}\text{Cl}_{0.06}]^-$ (symmetry code: (i) $-x+1, -y+2, -z+1$; (ii) $-x+1, -y+1, -z+1$): Hg1–N7 2.106(3), Hg1–N1 2.122(3), Hg1–N4 2.460(2), Hg1–Cl1 2.48(2), Hg1–N4ⁱ 2.580(2), Hg1–N1ⁱⁱ 2.976(2), N1–N2 1.205(3), N2–N3 1.151(3), N4–N5 1.193(3), N5–N6 1.154(3), N7–N8 1.191(6), N8–N9 1.140(5). $[\text{Ph}_4\text{P}][\text{Hg}(\text{N}_3)_{1.84}\text{Cl}_{1.16}]^-$ (symmetry code: (i) $-x+1, -y+2, -z+1$): Hg1–N1 2.132(7), Hg1–N4 2.1327(19), Hg1–Cl1 2.6657(5), Hg1–Cl1ⁱ 2.7763(5), Cl1–Hg1ⁱ 2.7763(5), N1–N2 1.209(6), N2–N3 1.154(5), N4–N5 1.195(3), N5–N6 1.147(3); $[\text{Ph}_4\text{P}][\text{Hg}(\text{N}_3)_{1.42}\text{Cl}_{2.58}]^{2-}$: Hg1–N4 2.22(2), Hg1–N1 2.258(5), Hg1–Cl1 2.423(8), Hg1–Cl2 2.529(9), N1–N2 1.178(8), N2–N3 1.170(9), N4–N5 1.18(2), N5–N6 1.13(2).

mercurates are neither shock, nor friction sensitive and deflagrate only gently in a flame. Albeit only small quantities of the tetrazolate crystals were observed during the crystallization in acetonitrile solutions, the formal [2+3] cycloaddition reaction between azido mercurate anions and acetonitrile should always be considered as possible source for impurities.



Scheme 4. Formation of diazido methyltetrazolato mercurate salt $[\text{PNP}][\text{Hg}(\text{N}_3)_2(\text{CH}_3\text{CN}_4)]$.

Physical and spectroscopic data

In contrast to binary cadmium and mercury(II) azide, none of the polyazido metallate salts $[\text{M}]_n[\text{E}(\text{N}_3)_{(2+n)}]$ as well as $[\text{Ph}_4\text{P}][\text{Cd}_2(\text{N}_3)_5(\text{H}_2\text{O})]$ and the DMSO adduct of $\text{Cd}(\text{N}_3)_2$ is sensitive to friction and shock. While crystalline α - and β - $\text{Hg}(\text{N}_3)_2$ are known to sublime at temperatures above 180 °C on gentle warming,^[5] pure $\text{Cd}(\text{N}_3)_2$ is found to detonate at about 345 °C on slow heating (20 °C min⁻¹) which compares well with the

value of 325 °C found by Wöhler et al. (Table 1).^[3e] However, it should be mentioned that the determination of the thermal detonation point of binary azides is in general strongly influenced by crystallite size, heating-rate and quantity.^[3e,5]

Contrary to binary $\text{Cd}(\text{N}_3)_2$, the adduct compound $\text{Cd}(\text{N}_3)_2 \cdot 3/2 \text{DMSO}$ does not explode, but melts at 120 °C. Likewise, $[\text{Ph}_4\text{P}][\text{Cd}(\text{N}_3)_3]$ and $[\text{PNP}]_2[\text{Cd}(\text{N}_3)_4]$ are thermally robust and possess similar melting points of 198 and 201 °C, respectively, while the salt $[\text{Ph}_4\text{P}][\text{Cd}_2(\text{N}_3)_5(\text{H}_2\text{O})]$ even remains solid to above 266 °C in accord with the observation by Beck et al. (Table 1).^[8] For the tri- and tetraazido mercurate salts also remarkably high melting points in the range 119–197 °C are observed. Thereby, the substitution of one azide ligand in $[\text{PNP}][\text{Hg}(\text{N}_3)_3]$ by a methyltetrazolato anion in the structurally related $[\text{PNP}][\text{Hg}(\text{N}_3)_2(\text{CH}_3\text{CN}_4)]$ obviously shows only little effect on the melting point (119 vs. 122 °C). While $\text{Cd}(\text{N}_3)_2$, $\text{Cd}(\text{N}_3)_2 \cdot 3/2 \text{DMSO}$ and $[\text{Ph}_4\text{P}][\text{Cd}_2(\text{N}_3)_5(\text{H}_2\text{O})]$ are hygroscopic and slowly decompose in air, mercury(II) azide as well as crystalline tri- and tetraazido cadmate and mercurate salts, respectively, are neither air, nor moisture sensitive. All compounds are slightly sensitive to light and should therefore be handled and stored in absence of sunlight. All azide compounds were fully characterized by ¹⁴N, ¹³³Cd and ¹⁹⁹Hg NMR, IR and Raman spectroscopy, elemental analysis and single-crystal structure elucidation.^[16] Table 1 summarizes the characterization data of all considered cadmium and mercury azide compounds.

The ¹⁴N NMR spectra of all compounds (run in $[\text{D}_6]\text{DMSO}$ at 300 K) show two well-resolved resonances (Table 1) in accord with literature known values for covalently bound azido groups (e.g., –136 (43) and –253 ppm (480 Hz) for $[\text{Bi}(\text{N}_3)_4]^-$).^[18c,19] The observation of only one set of azide signals and the absence of a separate N_α resonance indicate strong quadrupole relaxation effects and a rapid ligand exchange on the NMR timescale.^[20] As expected, a medium-sharp signal at $\delta = -132$ – -133 ppm ($\Delta\nu_{1/2} = 116$ – 230 Hz) for the N_β atoms of the cadmium compounds, and –131 ppm ($\Delta\nu_{1/2} = 40$ – 51 Hz) for the N_β atoms in the mercury salts, is observed. Obviously the shift of the N_β -resonance is only slightly influenced by the degree of substitution in the series of azide compounds, with exception of the resonance of binary $\text{Hg}(\text{N}_3)_2$ which is slightly shifted to higher field –133 ppm ($\Delta\nu_{1/2} = 65$ Hz; $\delta = -135$, $\Delta\nu_{1/2} = 30$ Hz in D_2O). While the remarkably broadened $\text{N}_{\alpha/\gamma}$ -resonances of the cadmium species in the range –277– -284 ppm ($\Delta\nu_{1/2} = 530$ – 1200 Hz) indicate no identifiable dependence on the degree of substitution by azide ligands, the influence on the shift for the $\text{N}_{\alpha/\gamma}$ atoms in the mercury compounds is more pronounced. In the series $\text{Hg}(\text{N}_3)_2 > [\text{Hg}(\text{N}_3)_3]^- > [\text{Hg}(\text{N}_3)_4]^{2-}$, the $\text{N}_{\alpha/\gamma}$ resonance is shifted to higher field ($\delta = -261$ – -270 ppm), while the half-widths of the signals decline ($\Delta\nu_{1/2} = 690$ – 276 Hz).

Only negligible differences were found between spectra of the tri- and tetraazido mercurates for both different counter ions $[\text{Ph}_4\text{P}]^+$ and $[\text{PNP}]^+$, respectively, indicating only weak cation–anion interactions in solution. Contrary to the ¹⁴N data, the ¹³³Cd NMR spectra display a clear trend dependent on the degree of substitution. While the resonance of cadmium(II) azide at –580 ppm is found at highest field (cf. $\text{Cd}(\text{N}_3)_2$ in D_2O :

Table 1. Selected analytical data.^[a] For comparison, the data of [Ph₄P]N₃ and [PNP]N₃ are included.^[16a]

Cd	M.p. [°C]	¹³³ Cd NMR [ppm]	¹⁴ N NMR ^[a] [ppm]	IR $\nu_{as}(\text{N}_3)$ ^[b] [cm ⁻¹]	Raman $\nu_{as}(\text{N}_3)$ ^[c] [cm ⁻¹]
Cd(N ₃) ₂	345 ^[d]	-580 ^[e]	-133(200), -282(1100)	2096(s), 2055(s), 1987(w)	2165(5), 2134(5), 2102(7), 2096(7), 2080(7), 2044(9)
Cd(N ₃) ₂ · 3/2 DMSO	120	-	-	2051(s, broad)	2115(8), 2077(2), 2070(2), 2060(1)
[Ph ₄ P][Cd ₂ (N ₃) ₅ (H ₂ O)]	266	-540	-132(230), -277(1200)	2099(m), 2071(m), 2052(m), 2024(s)	2134(22), 2073(15), 2055(13), 2045(13), 2032(14)
[Ph ₄ P][Cd(N ₃) ₃]	198	-449	-133(170), -284(820)	2065(s), 2044(s), 2015(s)	2098(7), 2038(1), 2024(1)
[PNP][Cd(N ₃) ₃]	- ^[f]	-487	-133(154), -281(770)	-	-
[Ph ₄ P] ₂ [Cd(N ₃) ₄]	- ^[f]	-419	-133(116), -281(530)	-	-
[PNP] ₂ [Cd(N ₃) ₄]	201	-417	-133(160), -280(830)	2072(m), 2037(s)	2073(3), 2041(5)
Hg	M.p. [°C]	¹⁹⁹ Hg NMR [ppm]	¹⁴ N NMR ^[a] [ppm]	IR $\nu_{as}(\text{N}_3)$ ^[b] [cm ⁻¹]	Raman $\nu_{as}(\text{N}_3)$ ^[c] [cm ⁻¹]
α -Hg(N ₃) ₂	195–200 ^[g]	-1745 ^[h]	-133(65), -261(690)	2089(m), 2044(s)	2127(4), 2094(11), 2071(3)
[PNP][Hg(N ₃) ₂ (CH ₃ CN ₄)]	122	-1420	-131(51), -267(380) ^[i]	2059(m), 2038(s), 2026(s)	2062(16), 2042(15), 2030(14)
[Ph ₄ P][Hg(N ₃) ₃]	147	-1546	-131(47), -267(428)	2038(s), 2006(s)	2077(10), 2045(4), 2008(2)
[PNP][Hg(N ₃) ₃]	119	-1539	-131(46), -266(400)	2071(m), 2041(s), 2021(s), 2000(s)	2062(9), 2036(3)
[Ph ₄ P] ₂ [Hg(N ₃) ₄]	143	-1407	-131(40), -270(300)	2049(m), 2007(s)	2054(10), 2020(4), 2010(3), 2001(3)
[PNP] ₂ [Hg(N ₃) ₄]	197	-1387	-131(40), -270(276)	2050(w), 2007(s)	2050(1), 2026(1), 2014(1)
[PNP]N ₃	214	-	-131(15), -277(25)	2004(m), 1989(s)	n.o. ^[j]
[Ph ₄ P]N ₃	235	-	-131(18), -276(52)	1993(s)	n.o. ^[j]

[a] Values from [D₆]DMSO, in parenthesis $\Delta\nu_{1/2}$ values in Hz. [b] Relative IR intensities denoted as weak (w), medium (m), strong (s). [c] Relative Raman intensities scaled to 100. [d] Detonation. [e] Cd(N₃)₂ in D₂O: ¹³³Cd: $\delta = -633$ ppm; ¹⁴N NMR $\delta = -133(39)$, -281 ppm (360). [f] Not isolated. [g] Sublimation (no decomposition up to 360 °C). [h] Hg(N₃)₂ in D₂O: ¹⁹⁹Hg NMR $\delta = -1785$ ppm; ¹⁴N NMR $\delta = -135$ (30), -265 ppm (400). [i] 2-Methyltetrazolate: ¹H-¹⁵N-HMBC $\delta = -80$ (CH₃CN₂N₂), 8.3 ppm (CH₃CN₂N₂). [j] Not observed; not Raman active due to almost ideal $D_{\infty h}$ symmetry

-633; CdCl₂: -586 ppm in water),^[21a,b] the pentaazido dicadmiate [Cd₂(N₃)₅(H₂O)]⁻ (-540 ppm), followed by the triazido- [M][Cd(N₃)₃] ([M]⁺ = [Ph₄P]⁺: -449; [PNP]⁺: -487 ppm) and tetraazido cadmates [M]₂[Cd(N₃)₄] ([M]⁺ = [Ph₄P]⁺: -419; [PNP]⁺: -417) become more deshielded. The ¹⁹⁹Hg NMR spectra of the mercury(II) azides also exhibit always one sharp signal, which is shifted to low field in the sequence Hg(N₃)₂ (-1745), [M][Hg(N₃)₃] ([M]⁺ = [Ph₄P]⁺: -1546; [PNP]⁺: -1539 ppm) and [M]₂[Hg(N₃)₄] ([M]⁺ = [Ph₄P]⁺: -1407; [PNP]⁺: -1387 ppm) following the opposite trend as observed in the ¹⁴N spectra (vide supra). This trend is in agreement with values found for the series HgCl₂ (-1560 ppm), [HgCl₃]⁻ (-1436 ppm) and [HgCl₄]²⁻ (-1152 ppm) in water.^[22] It is interesting to note, that the Hg resonance in the tetrazolate substituted compound [Hg(N₃)₂(CH₃CN₄)]⁻ is considerably low-field shifted (-1420 ppm) as compared to the corresponding triazido mercurate [Hg(N₃)₃]⁻ (-1539 ppm), which might indicate an additional deshielding by the aromatic tetrazolate ring. However, the opposite trend upon substitution of azide groups by methyltetrazolate units was observed by Klapötke et al. in the neutral organomercury azides RHgN₃ (cf. PhHgN₃: -1292 vs. PhHg(CH₃CN₄): -1324 ppm and CH₃HgN₃: -959 vs. CH₃Hg(CH₃CN₄): -980 ppm in [D₄]methanol).^[7f,g] It should be mentioned that the chemical shift in ¹³³Cd and ¹⁹⁹Hg NMR spectroscopy strongly depends on the concentration and polarity of the solvent (e.g., HgCl₂: -1560 in D₂O vs. -1502 in [D₆]DMSO; Hg(N₃)₂: -1785 in D₂O vs. -1745 ppm in [D₆]DMSO).^[21]

The vibrational spectra (ATR-IR/Raman) of cadmium and mercury compounds feature the presence of azido ligands as indicated by the antisymmetric stretching mode ($\nu_{as}(\text{N}_3)$; Cd: 2165–2024; Hg: 2127–2000 cm⁻¹, Table 1), the symmetric

stretching mode ($\nu_s(\text{N}_3)$; Cd: 1367–1331; Hg: 1373–1265 cm⁻¹), and the deformation mode of the N₃-unit ($\gamma/\delta(\text{N}_3)$; Cd: 667–594; Hg: 678–576 cm⁻¹). The existence of more than one azido ligand results in in-phase (i.p.) and out-of-phase (o.p.) coupling of vibrational modes in accord with theoretical data (Table 1 and Figure 5).^[1,16] Moreover, the combination mode of antisymmetric and symmetric vibration $\nu_{as} + \nu_s(\text{N}_3)$ can be found in the IR spectra (Cd: 3405–3302; Hg: 3309–3253 cm⁻¹). As illustrated in Figure 5, the $\nu_{as}(\text{N}_3)$ in the series Hg(N₃)₂ > [Hg(N₃)₃]⁻ > [Hg(N₃)₄]²⁻ is shifted to lower wave numbers, thereby indicating an increasingly ionic bonding situation to the azide groups, in accord with our calculations (vide infra).^[16] In the analogous cadmium compounds, the trend is less pronounced, which can be rationalized by the fact, that except of the tetraazido cadmates, which are distorted tetrahedrally coordinated, all other Cd compounds are six-coordinated in the solid state, leading to a higher degree of ionicity in the cadmium nitrogen bonds. It is worth mentioning, that our vibrational data of binary cadmium(II) azide agree well with the values reported by Schnick et al.^[10b]

Interestingly, the in-phase and out-of-phase N-Cd-N stretching modes ($\nu_{i.p.}/\nu_{o.p.}(\text{N-Cd-N})$) in the range 329–248 cm⁻¹ are observed at considerably lower wave number than in the mercury compounds, which indicates a stronger bonding (higher degree of covalent bonding) in the mercury(II) azides as compared to the analogous cadmium compounds, in agreement with our expectations. For the polyazido mercurate salts, only the in-phase N-Hg-N stretching mode ($\nu_{i.p.}(\text{N-Hg-N})$) in the range 373–331 cm⁻¹ is found, while for binary α -Hg(N₃)₂ both, the out-of-phase ($\nu_{o.p.}(\text{N-Hg-N})$; 434 and 420 cm⁻¹) as well as the in-phase vibrational mode ($\nu_{i.p.}(\text{N-Hg-N})$) at 349 cm⁻¹ can be identified in the Raman spectra. However, while these

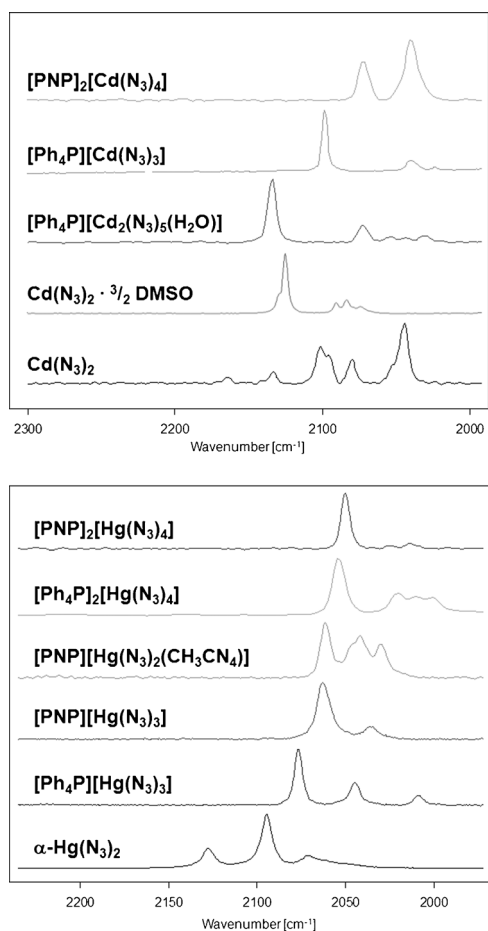


Figure 5. Antisymmetric stretching modes (Raman spectra) of the N_3 units ($\nu_{as}(N_3)$). Top: $Cd(N_3)_2$, $Cd(N_3)_2 \cdot 3/2 DMSO$, $[Ph_4P][Cd_2(N_3)_5(H_2O)]$, $[Ph_4P][Cd(N_3)_3]$ and $[PNP]_2[Cd(N_3)_4]$. Bottom: $\alpha-Hg(N_3)_2$, $[Ph_4P][Hg(N_3)_2]$, $[PNP][Hg(N_3)_3]$, $[PNP][Hg(N_3)_2(CH_3CN_4)]$, $[Ph_4P]_2[Hg(N_3)_4]$ and $[PNP]_2[Hg(N_3)_4]$.

values agree well with the IR data published by Dehnicke et al., it should be noted that the $\nu_{i.p.}(N-Hg-N)$ mode was erroneously assigned by the latter.^[3a] As expected, $[PNP][Hg(N_3)_2(CH_3CN_4)]$ exhibits also the typical antisymmetric (Raman: $\nu_{as}(N_3) = 2062(1), 2042(1), 2030 \text{ cm}^{-1}(1)$) as well as symmetric vibrational modes (Raman: $\nu_s(N_3) = 1388(1), 1322(1), 1278 \text{ cm}^{-1}(1)$) for the azide moieties. In addition, a strong N-N ring vibration at 1274 (s) (IR, cf. Raman: $1278 \text{ cm}^{-1}(1)$) is observed.

X-ray crystallography

The single crystal X-ray structures of all synthesized cadmium and mercury azide compounds, except $[PNP][Cd(N_3)_3]$, which was found to be inaccessible in the solid state (vide supra), and, moreover, the structures of the starting materials $[PNP][CdI_3]$, $[PNP]_2[CdI_4]$, $[Ph_4P][HgI_3]$ and $[Ph_4P]_2[HgI_4]$ were determined.

The crystallographic data are summarized in the Supporting Information (Tables S1–S8). As depicted in Figure 3, well separated $[E(N_3)_4]^{2-}$ anions are found in the $[Ph_4P]^+$ and $[PNP]^+$ salts of the tetraazido cadmates and mercurates, respectively.

The closest metal–metal distances are found in the $[Ph_4P]^+$ salts, with similar values for the cadmium and mercury compounds ($Cd \cdots Cd$ 7.436, $Hg \cdots Hg$ 7.482 Å), while the steric demand of the $[PNP]^+$ cation enforces considerably larger E–E distances ($Cd \cdots Cd$ 11.49, $Hg \cdots Hg$ 12.10 Å). In contrast, the structural units in the formal triazido metallate anions $[E(N_3)_3]^-$, as well as the formal pentaazido dicadmiate anion $[Cd_2(N_3)_5]^-$ and the DMSO solvate of $Cd(N_3)_2$ (Figure 1, Figure 2 and Figure 6), are considerably associated, forming one-dimensional chains in the solid state (Figure 7 and Figure 8).

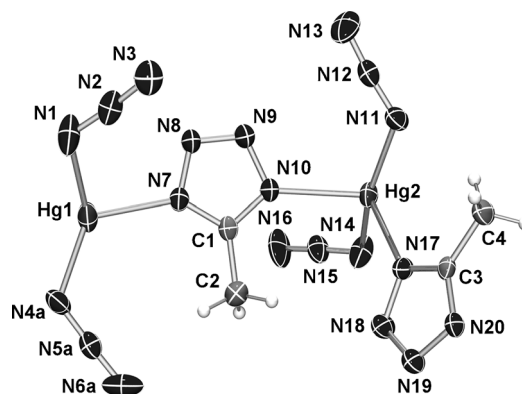


Figure 6. ORTEP drawing of the asymmetric unit of the $[Hg(N_3)_2(CH_3CN_4)]^-$ anion in the crystal. Thermal ellipsoids with 50% probability at 173 K. Disordered N_3 unit not displayed. Selected bond lengths [Å]: $Hg1-N4a$ 2.088(17), $Hg1-N1$ 2.237(5), $Hg1-N7$ 2.260(3), $Hg1-N20^i$ 2.275(4), $Hg2-N11$ 2.102(4), $Hg2-N14$ 2.123(4), $Hg2-N10$ 2.392(4), $Hg2-N17$ 2.397(4), $N1-N2$ 1.188(6), $N2-N3$ 1.159(6), $N4a-N5a$ 1.199(5), $N5a-N6a$ 1.151(5), $N7-C1$ 1.325(5), $N7-N8$ 1.356(5), $N8-N9$ 1.286(5), $N9-N10$ 1.360(5), $N10-C1$ 1.327(5), $N11-N12$ 1.200(4), $N12-N13$ 1.151(5), $N14-N15$ 1.199(5), $N15-N16$ 1.139(5), $N17-C3$ 1.323(5), $N17-N18$ 1.350(5), $N18-N19$ 1.303(5), $N19-N20$ 1.357(5), $N20-C3$ 1.324(6), $N20-Hg1^{ii}$ 2.275(4). Symmetry codes: (i) $x-1, y, z$; (ii) $x+1, y, z$.

With the exception of the tetraazido cadmate salts $[M]_2[Cd(N_3)_4]$, which display the anions in a slightly distorted tetrahedral ligand sphere with average N–Cd–N angles in the range $101.6\text{--}115.4^\circ$ (Table 2), all other cadmium azides are composed of six-coordinated cadmium centers, resembling slightly distorted octahedral coordination polyhedra with N–Cd–N angles averaging to the ideal value of 90° ($Cd(N_3)_2 \cdot 3/2 DMSO$ $76.4\text{--}107.0$, $[Ph_4P][Cd_2(N_3)_5(H_2O)]$ $78.3\text{--}101.8$, $[Ph_4P][Cd(N_3)_3]$ $82.6\text{--}97.4^\circ$, cf. $75.7\text{--}99.7^\circ$ in $Cd(N_3)_2$).^[10b]

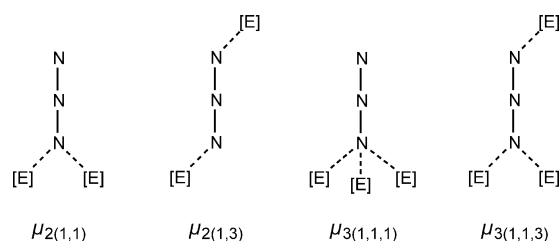
Accordingly, short Cd–Cd distances are found ($Cd(N_3)_2 \cdot 3/2 DMSO$ $3.585\text{--}3.689$, $[Ph_4P][Cd_2(N_3)_5(H_2O)]$ $3.523\text{--}3.697$, $[Ph_4P][Cd(N_3)_3]$ 3.637 Å, Figure 1) which lie only slightly above the sum of the van der Waals radii ($\sum r_{vdW}(Cd-Cd) = 3.20$ Å,^[23] cf. $Cd \cdots Cd$ in $Cd(N_3)_2$ 3.689 Å).^[10b] Within these structures, the octahedral units are either connected by $\mu_{2(1,1)}$ - or $\mu_{3(1,1,1)}$ -bridging azide ligands (Scheme 5), leading to common edge-sharing between two or three octahedra, respectively.

In the structure of $Cd(N_3)_2 \cdot 3/2 DMSO$, these interactions lead to the formation of tetrameric units consisting of four triply edge-sharing octahedra. These units are further connected to the adjacent units by $\mu_{2(1,1)}$ -bridging azide ligands, resulting in the formation of one-dimensional chains along [100] (Figure 1

Table 2. Selected structural data from single crystal X-ray determinations. Bond lengths in Å, angles in °.

Cd	Cd...Cd ^[a]	X-Cd-X (X=N, O)	Cd-O ^[b]	Cd-N	N _α -N _β	N _β -N _γ	N _α -N _β -N _γ
Cd(N ₃) ₂ ^[c]	3.689 ^[d]	75.7–99.7	–	2.348 μ _{3(1,1,3)} ^[e]	1.195	1.147	178.4
Cd(N ₃) ₂ ²⁻ /3 DMSO	3.585–3.689	76.4–107.0	2.289	2.302 μ _{2(1,1)} , 2.427 μ _{3(1,1,1)}	1.200, 1.219	1.146, 1.138	178.9, 179.3
[Ph ₄ P][Cd ₂ (N ₃) ₅ (H ₂ O)]	3.523–3.697	78.3–101.8	2.302	2.285, 2.292 μ _{2(1,1)} , 2.385 μ _{3(1,1,1)}	1.182, 1.193, 1.226	1.154, 1.145, 1.140	177.6, 178.3, 179.7
[Ph ₄ P][Cd(N ₃) ₃]	3.637	82.6–97.4	–	2.351 μ _{2(1,1)} , 2.377 μ _{2(1,3)}	1.204, 1.179	1.145, 1.177	178.9, 179.2
[Ph ₄ P] ₂ [Cd(N ₃) ₄]	7.436	101.6–115.4	–	2.191	1.184	1.139	175.2
[PNP] ₂ [Cd(N ₃) ₄]	11.49	102.9–110.8	–	2.193	1.175	1.147	174.4
Hg	Hg...Hg ^[a]	N-Hg-N ^[f,g]	Hg-N _{tetrazole}	Hg-N _{azid}	N _α -N _β	N _β -N _γ	N _α -N _β -N _γ
α-Hg(N ₃) ₂	4.377–4.566	173.0	–	2.062 μ _{3(1,1,3)}	1.217	1.141	175.1
[Ph ₄ P][Hg(N ₃) ₃]	3.888/4.161	158.3/78.9/98.3 ^[e]	–	2.105 ax., ^[g] 2.517 μ _{2(1,1)} , eq.	1.208, 1.199	1.145, 1.154	174.9, 179.2
[PNP][Hg(N ₃) ₃]	6.458/6.811	159.5/95.0/96.8	–	2.083 ax., 2.476 μ _{2(1,3)} , eq.	1.195, 1.168	1.133, 1.168	173.5, 180.0
[PNP][Hg(N ₃) ₂ (CH ₃ CN ₄) ^[h]]	6.706/6.765	157.1/104.9/97.5	2.331 μ _{2(1,3)} , eq.	2.154 ax.	1.196	1.149	174.5
[Ph ₄ P] ₂ [Hg(N ₃) ₄]	7.482	126.9/105.3/105.7	–	2.186 ax., 2.295 equiv	1.200, 1.193	1.152, 1.154	176.0, 176.5
[PNP] ₂ [Hg(N ₃) ₄]	12.10	131.6/108.1/104.0	–	2.180 ax., 2.286 equiv	1.190, 1.183	1.143, 1.160	174.8, 177.4

[a] Closest E...E distances. [b] If there are more than one azide, tetrazolate or DMSO ligands, the average value is given. [c] Values taken from Ref. [10b]. [d] Distance between edge-sharing CdN₆ polyhedra, an additional distance of 4.184 Å is found between corner-sharing CdN₆ polyhedra. [e] μ_{n(k,l,m)} denotes the bridging mode of the N₃ unit according to Scheme 5. [f] The angles are listed in the order N_{ax}-Hg-N_{ax}, N_{eq}-Hg-N_{eq} and average of N_{ax}-Hg-N_{eq}. [g] Refers to the axial or equatorial positions in the distorted tetrahedral ligand sphere (Scheme 6). [h] Disordered N₃ unit was not considered for mean values.



Scheme 5. Observed bridging modes of the azide units (E = Cd, Hg).

and Figure 7). Between these polymeric units, only weak N_γ...H_{DMSO} interactions are found all within the sum of the van der Waals radii. The closest N...H distance amounts to 2.457 Å (cf. Σr_{vdW}(N-H) 3.00 Å).^[23] The same μ_{2(1,1)} or μ_{3(1,1,1)}-bridging mode, as observed before, is found in the structure of [Ph₄P][Cd₂(N₃)₅(H₂O)], but contrarily, each octahedron is connected to each of the four neighboring octahedra by μ_{3(1,1,1)}-bridging azide ligands, resulting in a linear oriented double strand along [100], surrounded by the [Ph₄P]⁺ cations (Figure 1 and Figure 7). It is interesting to note, that the [Cd₂(N₃)₅(H₂O)]⁻ anion is isostructural to the analogue tetramethylammonium pentaazido dizincate anion in the salt [Me₄N][Zn₂(N₃)₅(H₂O)] published by Mautner et al.^[24] In the solid-state structure of [Ph₄P][Cd(N₃)₃], besides μ_{2(1,1)}-bridging azide ligands, leading to the formation of a straight assembly of edge sharing octahedra along [100], an additional μ_{2(1,3)}-bridging mode of azide units between adjacent Cd centers is observed, resulting in an alternating tilting of the octahedral coordination polyhedra (Figure 1 and Figure 7).

As illustrated in Table 2, the Cd–N and N–N distances vary strongly dependent on the coordination mode of the azide units. Accordingly, the shortest Cd–N distances are found for the single bonded, terminal azide groups in the tetraazido cadmates [M]₂[Cd(N₃)₄] with average Cd–N bond lengths of 2.191 Å ([M]⁺ = [Ph₄P]⁺) and 2.193 Å ([M]⁺ = [PNP]⁺), which lie slightly

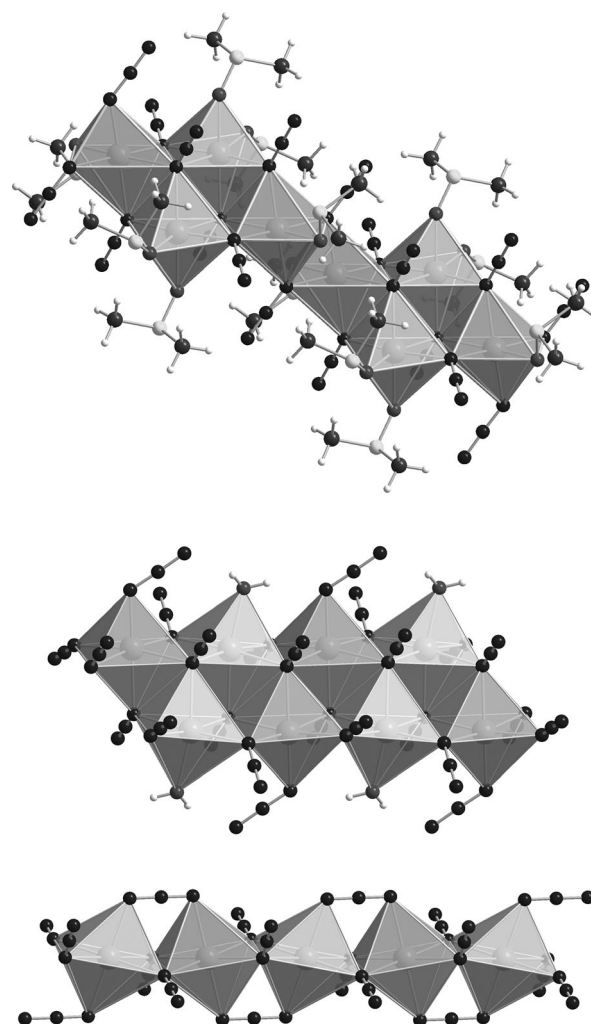


Figure 7. Side views of the one dimensional chains in the crystal. Top: Cd(N₃)₂²⁻/3 DMSO (view along [010]). Middle: [Ph₄P][Cd₂(N₃)₅(H₂O)] (view along [001]). Bottom: [Ph₄P][Cd(N₃)₃] (view along [001]). [Ph₄P]⁺ cations not displayed.

above the sum of the covalent radii for a cadmium nitrogen single bond ($\Sigma r_{\text{cov}}(\text{Cd-N}) = 2.07 \text{ \AA}$), but within the sum of the ion radii ($\Sigma r_{\text{ion}}(\text{Cd-N}) = 2.24 \text{ \AA}$) for a tetrahedral coordination sphere.^[25,23] The azide units adopt a typical *trans*-bent structure with short average $\text{N}_\alpha\text{-N}_\beta$ and $\text{N}_\beta\text{-N}_\gamma$ distances (1.184 and 1.139 \AA in $[\text{Ph}_4\text{P}]_2[\text{Cd}(\text{N}_3)_4]$, 1.175 and 1.147 \AA in $[\text{PNP}]_2[\text{Cd}(\text{N}_3)_4]$) and $\text{N}_\alpha\text{-N}_\beta\text{-N}_\gamma$ angles which deviate considerably from linearity ($[\text{Ph}_4\text{P}]_2[\text{Cd}(\text{N}_3)_4]$ 175.2, $[\text{PNP}]_2[\text{Cd}(\text{N}_3)_4]$ 174.4°).

In contrast, the Cd–N length to the terminal azide ligand in the octahedral coordination sphere of the cadmium center in the $[\text{Cd}_2(\text{N}_3)_5(\text{H}_2\text{O})]^-$ anion is considerably elongated (2.285(2) \AA), in accord with the sum of the ionic radii $\Sigma r_{\text{ion}}(\text{Cd-N})$ of 2.41 \AA for an octahedral coordination sphere.^[23] This, together with the slightly longer $\text{N}_\alpha\text{-N}_\beta$ and $\text{N}_\beta\text{-N}_\gamma$ distances of 1.182(3) and 1.154(3) \AA , respectively, and a flat angle of 177.6° indicate a higher degree of ionic bonding. In the same way, the Cd–N bond lengths to the μ_2 and μ_3 -bridging azide units are considerably elongated ($\text{Cd}(\text{N}_3)_2 \cdot 3/2 \text{ DMSO}$ $\mu_{2(1,1)}$ 2.302, $\mu_{3(1,1)}$ 2.427, $[\text{Ph}_4\text{P}][\text{Cd}_2(\text{N}_3)_5(\text{H}_2\text{O})]$ $\mu_{2(1,1)}$ 2.292, $\mu_{3(1,1)}$ 2.385, $[\text{Ph}_4\text{P}][\text{Cd}(\text{N}_3)_3]$ $\mu_{2(1,1)}$ 2.351 \AA , cf. $\mu_{3(1,1)}$ 2.348 \AA in $\text{Cd}(\text{N}_3)_2$.^[10b] The $\text{N}_\alpha\text{-N}_\beta$ and $\text{N}_\beta\text{-N}_\gamma$ distances follow the same trend, with the longest Cd–N and N–N bonds as well as largest $\text{N}_\alpha\text{-N}_\beta\text{-N}_\gamma$ angles found for the triply $\mu_{3(1,1)}$ -bridging azides (Table 2). While the terminal coordinated bridging azide units always exhibit $\text{N}_\alpha\text{-N}_\beta$ bond lengths, which are longer than the $\text{N}_\beta\text{-N}_\gamma$ bonds, in the $[\text{Cd}(\text{N}_3)_3]^-$ anion two almost equal distances of 1.179 and 1.177 \AA are observed in the $\mu_{2(1,3)}$ -bridging azide ligand (cf. $\text{N}_\alpha\text{-N}_\beta/\gamma$ 1.171–1.176 \AA in $[\text{Me}_4\text{N}][\text{Cd}(\text{N}_3)_3]$.^[14b] The mean Cd–O bond length of 2.289 \AA in $\text{Cd}(\text{N}_3)_2 \cdot 3/2 \text{ DMSO}$, and the Cd–O bond to the water molecule in $[\text{Ph}_4\text{P}][\text{Cd}_2(\text{N}_3)_5(\text{H}_2\text{O})]$ with 2.302 \AA are considerably longer than the sum of the covalent radii $\Sigma r_{\text{cov}}(\text{Cd-O}) = 1.99$ ^[25] but in accord with the sum of ionic radii $\Sigma r_{\text{ion}}(\text{Cd-O})$ of 2.30 \AA ^[23] (cf. $\Sigma r_{\text{vdw}}(\text{Cd-O})$ 3.10 \AA).^[23] In the polyazido cadmate salts, only weak N...H interactions between the anions and cations ($[\text{Ph}_4\text{P}][\text{Cd}(\text{N}_3)_3]$ 2.618, $[\text{Ph}_4\text{P}][\text{Cd}_2(\text{N}_3)_5(\text{H}_2\text{O})]$ 2.599, $[\text{Ph}_4\text{P}]_2[\text{Cd}(\text{N}_3)_4]$ 2.439, $[\text{PNP}]_2[\text{Cd}(\text{N}_3)_4]$ 2.517 \AA), within the sum of the van der Waals radii of $\Sigma r_{\text{vdw}}(\text{N-H})$ 3.00 \AA are observed in the solid state.^[23] However, the closest intramolecular N...H contacts are found between the water molecule and the adjacent terminal azide groups in $[\text{Ph}_4\text{P}][\text{Cd}_2(\text{N}_3)_5(\text{H}_2\text{O})]$, with donor–acceptor distances (D–H...A) of 2.879 and 2.919 \AA (cf. $\Sigma r_{\text{vdw}}(\text{N-O})$ 3.10 \AA ,^[23] Figure 1).

In analogy to the cadmium compounds, the triazido mercurate $[\text{Hg}(\text{N}_3)_3]^-$ and diazido tetrazolato mercurate $[\text{Hg}(\text{N}_3)_2(\text{CH}_3\text{CN}_4)]^-$ anions, respectively, are also aggregated in the solid state, forming one-dimensional polyanionic chains, surrounded by the $[\text{Ph}_4\text{P}]^+$ or $[\text{PNP}]^+$ cations (Figure 2 and Figure 8). However, the Hg^{2+} cations in all azide compounds adopt a strongly distorted tetrahedral coordination geometry (Figure 2, Figure 3 and Figure 8).

In $[\text{Ph}_4\text{P}][\text{Hg}(\text{N}_3)_3]$, the triazido mercurate anions are associated by two $\mu_{2(1,1)}$ -bridging azide ligands, resulting in the formation of a centrosymmetric $[\text{Hg}_2(\text{N}_3)_6]^{2-}$ dianion, which resembles two tetrahedral coordination polyhedra, sharing one common edge. These dimers are further connected to adjacent units via weak intermolecular $\text{Hg}\cdots\text{N}$ interactions just below the sum of the van der Waals radii (Hg1-N^{ii} 2.966 \AA , cf.

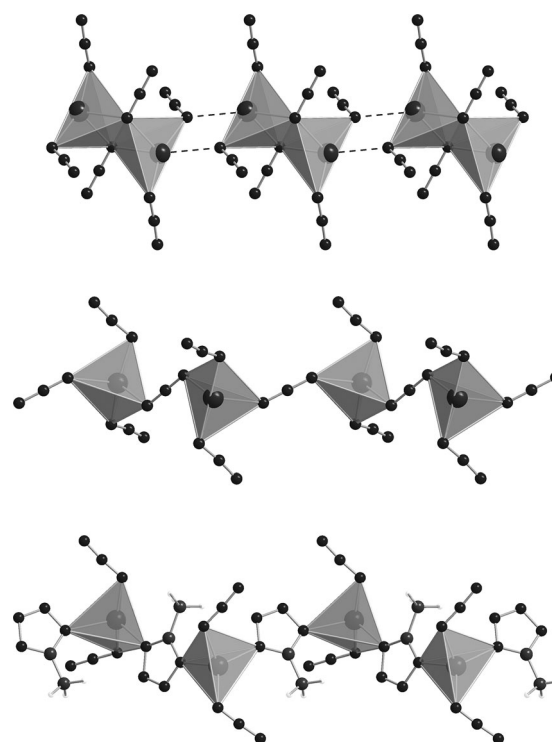
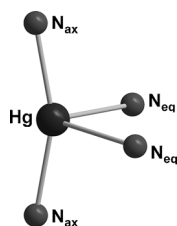


Figure 8. Side views of the one dimensional chains in the crystal. Top: $[\text{Ph}_4\text{P}][\text{Hg}(\text{N}_3)_3]$ (view along $[001]$). Middle: $[\text{PNP}][\text{Hg}(\text{N}_3)_3]$ (view along $[010]$). Bottom: $[\text{PNP}][\text{Hg}(\text{N}_3)_2(\text{CH}_3\text{CN}_4)]$ (view along $[001]$). $[\text{Ph}_4\text{P}]^+$ and $[\text{PNP}]^+$ cations not displayed.

$\Sigma r_{\text{vdw}}(\text{Hg}\cdots\text{N}) = 3.10 \text{ \AA}$,^[23] Figure 8), resulting in a zig-zag chain along $[100]$. The $\text{Hg}\cdots\text{Hg}$ distance amounts to 3.888 \AA within the dimercurate anions, and 4.161 \AA between neighboring dimers (cf. $\text{Hg}\cdots\text{Hg}$ 4.377–4.566 \AA in $\alpha\text{-Hg}(\text{N}_3)_2$.^[5] In contrary, in the $[\text{PNP}]^+$ salts of the triazido mercurate and its tetrazolato derivative, the tetrahedral coordination polyhedra are less associated. While the mercurate units in $[\text{PNP}][\text{Hg}(\text{N}_3)_3]$ are connected via shared $\mu_{2(1,3)}$ -bridging azide ligands ($\text{Hg}\cdots\text{Hg}$ 6.458 and 6.811 \AA), a similar coordination geometry is induced by the 1,3-bridging mode of the 2-methyl-tetrazolate units resulting in the formation of polyanionic chains along $[100]$, with $\text{Hg}\cdots\text{Hg}$ distances of 6.706 and 6.765 \AA . Obviously, the bulky $[\text{PNP}]^+$ cations induce a considerable amount of strain within the mercurate units, leading to a stronger separation of mercury centers.

In accord with our calculations (vide infra), always two shorter and two clearly longer Hg–N bond lengths are observed within the HgN_4 coordination spheres, which comply with the axial and equatorial ligands in a strongly distorted tetrahedral geometry as depicted in Scheme 6 ($[\text{Ph}_4\text{P}][\text{Hg}(\text{N}_3)_3]$ ax. 2.105, eq. 2.517, $[\text{PNP}][\text{Hg}(\text{N}_3)_3]$ ax. 2.083, eq. 2.476, $[\text{PNP}][\text{Hg}(\text{N}_3)_2(\text{CH}_3\text{CN}_4)]$ ax. 2.154, $[\text{Ph}_4\text{P}]_2[\text{Hg}(\text{N}_3)_4]$ ax. 2.186, eq. 2.295, $[\text{PNP}]_2[\text{Hg}(\text{N}_3)_4]$ ax. 2.180, eq. 2.286 \AA , cf. ax. 2.062 in $\alpha\text{-Hg}(\text{N}_3)_2$.^[5] Table 2). These values lie slightly above the sum of the covalent radii ($\Sigma r_{\text{cov}}(\text{Hg-N}) = 2.04 \text{ \AA}$),^[25] but within the sum of the ionic radii $\Sigma r_{\text{ion}}(\text{Hg-N}) = 2.42 \text{ \AA}$.^[23] The average Hg–N bond length between the mercury center and the nitrogen atoms of the $\mu_{2(1,3)}$ -bridging tetrazolato ligand equals to

2.331 Å (cf. 2.113 Å in MeHg(CH₃CN₄)).^[79] As displayed in Table 2, the Hg–N bond lengths increase continuously along the series α -Hg(N₃)₂ > [Ph₄P][Hg(N₃)₃] > [PNP][Hg(N₃)₃] > [Ph₄P]₂[Hg(N₃)₄] > [PNP]₂[Hg(N₃)₄], in accord with an increasing ionic bond situation. Interestingly, in the tri- and tetraazido mercurates the shortest Hg–N bonds are always found in the corresponding [PNP]⁺ salts. With the exception of the $\mu_{2(1,3)}$ -bridging azide units in [PNP][Hg(N₃)₃], which are ideal linear (N–N–N 180°), and feature an average N–N bond length of 1.168 Å, the typical *trans*-bent structure is observed for all



Scheme 6. Distorted tetrahedral coordination environment in the mercury azide compounds (ax = axial, eq = equatorial).

other azide ligands, with considerably different N_α–N_β and N_α–N_γ bond distances and N_α–N_β–N_γ angles which differ considerably from linearity (Table 2). As with the analogous cadmium compounds, only weak N...H interactions are observed between the anions and cations in the polyazido mercurate salts, ([Ph₄P][Hg(N₃)₃] 2.456(2), [PNP][Hg(N₃)₃] 2.596(3), [PNP][Hg(N₃)₂(CH₃CN₄)] 2.44(2), [Ph₄P]₂[Hg(N₃)₄] 2.484(2), [PNP]₂[Hg(N₃)₄] 2.509(3) Å), which lie within the sum of the van der Waals radii of $\sum r_{vdW}(N-H)$ 3.00 Å.^[23]

Computational data

To shed some light on the structural diversity and bonding of E(N₃)₂, [E(N₃)₃][–], and [E(N₃)₄]^{2–} (E = Cd, Hg) species, a series of computations at the M06-2X level was carried out, addressing thermodynamic and structural questions. For this reason the gas phase thermodynamics of the successive anion formation upon adding N₃[–] to E(N₃)₂ was calculated (Table S32 in the Supporting Information). Additionally, it was our aim to study in detail the structural and electronic influence of the azido ligands. A summary of the structural data as well as the calculated NBO^[26–28] data are given in Table 3 and Table S33 in the Supporting Information.

Table 3. Net charges (<i>q</i>) and occupation numbers (<i>occ.</i>) in e.			
E = Cd	E(N ₃) ₂ ^[a]	[E(N ₃) ₃] ^{–[b]}	[E(N ₃) ₄] ^{2–[c]}
<i>q</i> (E)	1.49	1.61	1.67
<i>q</i> (N _α)	–0.83	–0.80	–0.72
<i>q</i> (N _β)	0.22	0.22	0.22
<i>q</i> (N _γ)	–0.14	–0.29	–0.42
<i>occ.</i> (5 s)	0.55	0.38	0.32
E = Hg	E(N ₃) ₂ ^[a]	[E(N ₃) ₃] ^{–[b]}	[E(N ₃) ₄] ^{2–[c]}
<i>q</i> (E)	1.28	1.44	1.53
<i>q</i> (N _α)	–0.75	–0.75	–0.69
<i>q</i> (N _β)	0.22	0.21	0.21
<i>q</i> (N _γ)	–0.11	–0.28	–0.40
<i>occ.</i> (6 s)	0.88	0.59	0.46

[a] *cis*-C₂ isomer. [b] *s*-C_{3h} isomer. [c] S₄ isomer.

For nitrogen an aug-cc-pVDZ basis set was used and for Cd and Hg a fully relativistic pseudopotential (Cd: ECP28 MDF, Hg: ECP60 MDF)^[29] and an aug-cc-pVDZ basis set (26s23p14d2f)/[5s5p4d2f]).^[30]



For the E(N₃)₂ species three configurations (*cis*-C_{2v}, *trans*-C_{2h}, and *cis*-C₂) were considered (Figure 9 and Figure S29 in the Supporting Information). As displayed in Figure S22 in the Supporting Information, the potential energy surfaces of all E(N₃)₂ species are very flat with respect to the position of the azido ligands to each other (*cis* vs. *trans*).

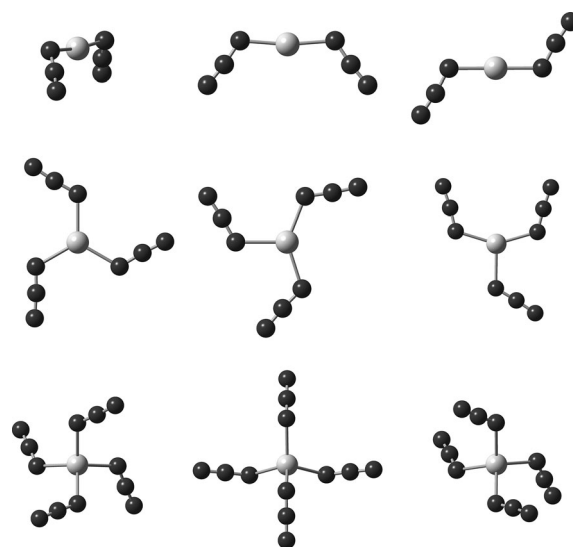


Figure 9. Computed structures of E(N₃)₂ (top: *cis*-C_{2v}, *cis*-C₂, and *trans*-C_{2h}), [E(N₃)₃][–] (*s*-C_{3h}, *s*-C₂, *y*-C₁), and [E(N₃)₄]^{2–} (S₄, D₂, and C₂ symmetry).

While the energies for the minimum structures *cis*-C_{2v} and *cis*-C₂ are almost identical, the *trans*-C_{2h} species is slightly less favored ($\Delta G_{298} < 2$ kcal mol^{–1}) and represents a transition state (NIMAG = 1, number of imaginary frequencies). All distances and angles of these three species differ only slightly, also indicating highly flexible azido ligands with respect to rotation about the Hg–N axis (very small rotational barriers), in accord with our experimental X-ray data (*vide infra*).

A very similar situation is found for the anionic complexes [E(N₃)₃][–] and [E(N₃)₄]^{2–}. For [E(N₃)₃][–] three different isomers are found: *y*-C₁, *s*-C₂ and *s*-C_{3h} (Figure 9), which all lie within 1 kcal mol^{–1} (relative energies). Interestingly, there is a difference between the Hg and Cd species for the two non-C_{3h} symmetric species. In *y*-C₁ and *s*-C₂-[Hg(N₃)₃][–], always one longer (2.25–2.26 Å) and two shorter Hg–N distances (2.153–2.163 Å) are observed along with one large N–Hg–N (140.8–146.7°) and two smaller N–Hg–N angles (106.5–111.6°), in accordance with X-ray data where such preformed Hg(N₃)₂ units are observed (e.g., [PNP][Hg(N₃)₃] Hg–N_{ax} 2.083, Hg–N_{eq} 2.476 Å, N_{ax}–Hg–N_{ax} 159.5,

$N_{\text{eq}}\text{-Hg-}N_{\text{eq}}$ 95.0°, vide supra). That is, these species can also be referred to as formal $\text{Hg}(\text{N}_3)_2[\text{M}]\text{N}_3$ species. For the analogous Cd species all Cd–N bond lengths and N–Cd–N angles are very similar and close to C_{3h} symmetry (Table S30 in the Supporting Information).

While for $[\text{Hg}(\text{N}_3)_4]^{2-}$ three different isomers (with C_2 , D_2 and S_4 symmetry) are found, only the C_2 and S_4 symmetric species are stable minima on the Cd potential energy surface. Again, all considered species are very similar in energy ($\Delta G_{298} < 1.2 \text{ kcal mol}^{-1}$) displaying highly flexible azido ligands with respect to their arrangement around the metal ion (Table S31 in the Supporting Information).

As expected, NBO analysis clearly indicates ionic bonding between formal E^{2+} and N_3^- ions. However, a closer look at the computed net charges and the occupation of the 5s (Cd) and 6s (Hg) orbitals, respectively, reveals small but significant differences between Hg and Cd species as well as along the series $E(\text{N}_3)_2$, $[\text{E}(\text{N}_3)_3]^-$, and $[\text{E}(\text{N}_3)_4]^{2-}$. Assuming ideal E^{2+} ions, empty 5s (Cd) and 6s (Hg) orbitals are expected. As displayed in Table 3, the computed occupation numbers of the valence s-type atomic orbitals are quite different from zero (Hg: between 0.465–0.88 e; Cd: 0.32–0.55 e) strongly decreasing along $E(\text{N}_3)_2 > [\text{E}(\text{N}_3)_3]^- > [\text{E}(\text{N}_3)_4]^{2-}$. In accordance with these findings, the computed positive net charges on E increase along this series (Hg: between 1.28–1.53 e; Cd: 1.49–1.67 e). Two things can be derived from these NBO data: 1) the (small) covalency in the E–N bond increases from Cd to Hg, but 2) decreases along $E(\text{N}_3)_2 > [\text{E}(\text{N}_3)_3]^- > [\text{E}(\text{N}_3)_4]^{2-}$. The ionic bonding between the formal E^{2+} and the azido ligands becomes clearly visible in the electron localization function (ELF), which also displays distorted lone pairs located on the N_α atoms (Figure 10 and Figure S22 in the Supporting Information) as well as a stronger core polarization for the Hg species compared to the Cd species.

The charge distribution in all azides is characterized by alternating net charges along the $M^{(\delta+)}\text{-N}^{(\delta-)}\text{-N}^{(\delta+)}\text{-N}^{(\delta-)}$ units. Interestingly, the positive net charge on N_β is almost constant in all species (Hg: 0.21–0.22 e, Cd: 0.22 e), the negative charge on N_α only slightly decreases along $E(\text{N}_3)_2 > [\text{E}(\text{N}_3)_3]^- > [\text{E}(\text{N}_3)_4]^{2-}$ and Cd species $>$ Hg species (Hg: –0.75––0.69 e, Cd: –0.72––0.83 e), while the terminal N_γ atoms feature a significant increase of negative charge along this series (Hg(N_3)₂: –0.11, $[\text{Hg}(\text{N}_3)_3]^-$: –0.25, $[\text{Hg}(\text{N}_3)_4]^{2-}$: –0.40 e; Cd(N_3)₂: –0.14, $[\text{Cd}(\text{N}_3)_3]^-$: –0.29, $[\text{Hg}(\text{N}_3)_4]^{2-}$: –0.42 e) which is also displayed by the difference in the ¹⁴N NMR shift of the N_γ atom (vide supra, Table 1).

Experimentally we could show, that salts bearing the $[\text{E}(\text{N}_3)_3]^-$ anion can be prepared from neutral $E(\text{N}_3)_2$ and N_3^- ions and in agreement with these results the gas phase Gibbs energies for this reaction [Eq. (1)] are all exergonic decreasing along $E = \text{Cd} < \text{Hg}$ (ΔG_{298} : –66.6 vs. –46.5 kcal mol^{–1}, Table S32 in the Supporting Information). However, the next step, the addition of a second azido ligand leading to the formation of the $[\text{E}(\text{N}_3)_4]^{2-}$ dianion [Eq. (2)], was computed to be endergonic in the gas phase with the same trend as discussed before, that is $[\text{Cd}(\text{N}_3)_4]^{2-}$ (+27.8 kcal mol^{–1}) is the more stable than the analogous Hg species (+35.9 kcal mol^{–1}). Consequential, it can be

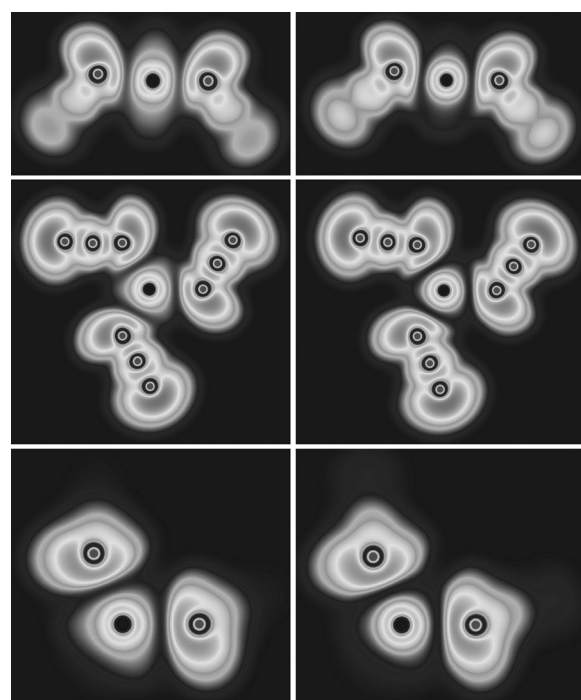


Figure 10. Two-dimensional cross-section through one molecule plane (including E) of the electron localization function (ELF). Left: Cd; right: Hg species; top: *cis*- C_2 - $E(\text{N}_3)_2$, middle: *s*- C_{3h} - $[\text{E}(\text{N}_3)_3]^-$, and bottom: S_4 - $[\text{E}(\text{N}_3)_4]^{2-}$.

assumed that solid state effects such as electrostatic interaction between cation and anion stabilizes salts bearing such dianions. However, the larger energy gain for the Cd species may explain the larger coordination number (in all cases six except from $[\text{Cd}(\text{N}_3)_4]^{2-}$), while the Hg species prefer four with often quite different Hg–N distances and a preformed $\text{Hg}(\text{N}_3)_2$ moiety.

Conclusion

In conclusion, we present here a comprehensive study of the $[\text{Ph}_4\text{P}]^+$ and $[\text{PNP}]^+$ salts of triazido and tetraazido cadmate and mercurate anions. All salts are easily accessible by means of iodide/azide exchange in polyiodo metallates with AgN_3 , or by direct reaction of the corresponding binary azide $E(\text{N}_3)_2$ with $[\text{M}]\text{N}_3$ in acetonitrile or DMSO. While the solid-state structures display the Hg^{2+} cations in a strongly distorted tetrahedral coordination environment, the cadmium(II) centers are octahedrally coordinated, with exception of the tetraazido cadmate anion, which builds almost ideal tetrahedral coordination polyhedra. In accord with our calculations, the bonding between the metal centers and the azide ligands can be referred to as dominantly ionic. In the Hg compounds, a considerable core polarization and a small covalent contribution in the Hg–N bonds, decreasing along $E(\text{N}_3)_2 > [\text{E}(\text{N}_3)_3]^- > [\text{E}(\text{N}_3)_4]^{2-}$ can be discussed. Moreover, possible side reactions during the synthesis of polyazido mercurates such as the chloride/azide exchange in CH_2Cl_2 , as well as the formation of mercury methyl-tetrazolate salts by formal [2+3]-cycloaddition with acetonitrile were observed. While comparative thermodynamic, vibrational

(IR/Raman) and NMR data of polyazido cadmates and mercurates could be obtained for the first time, the structural elucidation of $[\text{Hg}(\text{N}_3)_3]^-$ and $[\text{Hg}(\text{N}_3)_4]^{2-}$ salts fills an open gap in transition-metal chemistry.

Experimental Section

Caution! Covalent azides are potentially hazardous and can decompose explosively under various conditions! Especially $\text{Cd}(\text{N}_3)_2$ and $\text{Hg}(\text{N}_3)_2$ are extremely shock-sensitive and can explode violently upon the slightest provocation. Appropriate safety precautions (safety shields, face shields, leather gloves, protective clothing) should be taken when dealing with large quantities.

$\text{Cd}(\text{N}_3)_2$

To a stirred suspension of cadmium(II) fluoride CdF_2 (0.451 g, 3.0 mmol) in acetonitrile (5 mL), neat trimethylsilylazide, Me_3SiN_3 (1.728 g, 15.0 mmol) was added in one portion at ambient temperature. Stirring for 24 h under exclusion of light resulted in a colorless precipitate and a yellowish supernatant. The solid was collected by centrifugation (up to 450 g), the supernatant was removed by decantation and the resulting colorless precipitate was resuspended in 2 mL of acetonitrile. The washing procedure was repeated five times, until the supernatant was colorless. The residue was dried in vacuo at ambient temperature for one hour and was then carefully grounded by means of a plastic spatula. Heating for 2 h at 60–80 °C in vacuo yielded cadmium(II) azide $\text{Cd}(\text{N}_3)_2$ as a colorless solid, which was stored under argon at ambient temperature under exclusion of light (yield: 80–90%). M.p. 345 °C (detonation, heating-rate 20 °C min⁻¹ under argon); ¹³³Cd NMR (300 K, $[\text{D}_6]\text{DMSO}$, 111.00 MHz): $\delta = -580$ ppm ($\Delta\nu_{1/2} = 350$ Hz); ¹³³Cd NMR (300 K, D_2O , 111.00 MHz): $\delta = -633$ ppm ($\Delta\nu_{1/2} = 130$ Hz); ¹⁴N NMR (300 K, $[\text{D}_6]\text{DMSO}$, 36.14 MHz): $\delta = -133$ (N_{β} , $\Delta\nu_{1/2} = 200$ Hz), -282 ppm (N_{γ} , $\Delta\nu_{1/2} = 1100$ Hz); ¹⁴N NMR (300 K, D_2O , 36.14 MHz): $\delta = -133$ (N_{β} , $\Delta\nu_{1/2} = 39$ Hz), -281 ppm (N_{γ} , $\Delta\nu_{1/2} = 360$ Hz); IR (ATR, 32 scans): $\tilde{\nu} = 3405$ (w), 2752 (w), 2729 (w), 2674 (w), 2602 (w), 2096 (s), 2055 (s), 1987 (w), 1362 (m), 1313 (w), 1295 (w), 1226 (w), 1188 (w), 667 (m), 653 (m), 611 (w), 594 cm⁻¹ (w); Raman (784 nm, 21 mW, 25 °C, 5 acc., 60 s): $\tilde{\nu} = 2165$ (1), 2134 (1), 2102 (1), 2096 (1), 2080 (1), 2044 (1), 1367 (9), 1312 (1), 1295 (1), 665 (1), 651 (1), 617 (1), 609 (1), 595 (1), 314 (1), 271 (2), 213 (4), 181 (5), 151 (6), 117 (10), 102 (6), 77 (6), 68 cm⁻¹ (8).

$\text{Cd}(\text{N}_3)_2 \cdot 3/2 \text{DMSO}$

Cadmium(II) azide, $\text{Cd}(\text{N}_3)_2$ (0.04 g, 0.2 mmol) was dissolved in DMSO (0.4 mL) at ambient temperature. The colorless solution was concentrated in vacuo and a few drops of acetone were added slowly to initiate crystallization. Storage at ambient temperature for ten hours, resulted in the deposition of needle-like crystals. Removal of supernatant by syringe and drying in vacuo for one hour gave cadmium(II) azide DMSO solvate $\text{Cd}(\text{N}_3)_2 \cdot 3/2 \text{DMSO}$ as colorless crystals (yield: 70–90%). M.p. 120 °C; IR (ATR, 32 scans): $\tilde{\nu} = 3382$ (w), 3340 (w), 3005 (w), 2915 (w), 2638 (w), 2546 (w), 2451 (w), 2051 (s), 1435 (m), 1405 (m), 1343 (m), 1305 (m), 1293 (m), 1236 (m), 1209 (w), 1023 (s), 1007 (s), 995 (s), 953 (s), 938 (s), 904 (m), 707 (m), 674 (m), 658 (m), 633 (m), 605 cm⁻¹ (m); Raman (784 nm, 21 mW, 25 °C, 2 acc., 60 s): $\tilde{\nu} = 3011$ (1), 2918 (1), 2115 (1), 2077 (1), 2070 (1), 2060 (1), 1414 (1), 1348 (4), 1311 (2), 1296 (2), 1240 (2), 1210 (1), 1040 (2), 1030 (1), 1010 (2), 1002 (1), 958 (2), 940 (1), 714 (2), 708 (2), 679 (6), 383 (1), 360 (1), 341 (2), 315 (2), 232 (7),

138 cm⁻¹ (10); elemental analysis calcd (%) for $\text{C}_3\text{H}_9\text{N}_6\text{O}_{1.5}\text{CdS}_{1.5}$: Cd 35.84; found: Cd 35.77.

$[\text{Ph}_4\text{P}][\text{Cd}(\text{N}_3)_3]$

Procedure 1: To a stirred suspension of tetraphenylphosphonium triiodo cadmate $[\text{Ph}_4\text{P}][\text{CdI}_3]$ (0.416 g, 0.5 mmol) in acetonitrile (10 mL), silver azide AgN_3 (neat, 0.240 g, 1.60 mmol) was added in one portion at ambient temperature. The yellowish suspension was stirred for one hour and filtered (F4), resulting in a colorless solution. The solvent was removed in vacuo and the residue was dissolved in DMSO (0.6 mL). The colorless solution was allowed to evaporate over a period of two days resulting in the deposition of colorless needle-like crystals. The viscous supernatant was removed by decantation and the crystals were washed with a few drops of acetone and dried between two filter papers for five minutes. Drying in vacuo (5 mbar) over P_4O_{10} in a desiccator for 12 h gave tetraphenylphosphonium triazido cadmate $[\text{Ph}_4\text{P}][\text{Cd}(\text{N}_3)_3]$ as colorless crystals (yield: 50–60%).

Procedure 2: Cadmium(II) azide $\text{Cd}(\text{N}_3)_2$ (0.049 g, 0.25 mmol) and tetraphenylphosphonium azide $[\text{Ph}_4\text{P}]\text{N}_3$ (0.095 g, 0.25 mmol) were combined and dissolved in DMSO (0.6 mL) at ambient temperature. The colorless solution was allowed to evaporate over a period of two days resulting in the deposition of colorless needle-like crystals. The viscous supernatant was removed by decantation and the crystals were washed with a few drops of acetone and dried between two filter papers for five minutes. Drying in vacuo (5 mbar) over P_4O_{10} in a desiccator for 12 h gave tetraphenylphosphonium triazido cadmate $[\text{Ph}_4\text{P}][\text{Cd}(\text{N}_3)_3]$ as colorless crystals (yield: 50–60%); M.p. 198 °C; ¹³³Cd NMR (300 K, $[\text{D}_6]\text{DMSO}$, 111.00 MHz): $\delta = -449$ ppm ($\Delta\nu_{1/2} = 410$ Hz); ¹⁴N NMR (300 K, $[\text{D}_6]\text{DMSO}$, 36.14 MHz): $\delta = -133$ (N_{β} , $\Delta\nu_{1/2} = 170$ Hz), -284 ppm (N_{γ} , $\Delta\nu_{1/2} = 820$ Hz); IR (ATR, 32 scans): $\tilde{\nu} = 3369$ (w), 3350 (w), 3302 (w), 3079 (w), 3062 (w), 3051 (w), 3020 (w), 2991 (w), 2065 (s), 2044 (s), 2015 (s), 1585 (m), 1574 (w), 1482 (m), 1435 (s), 1334 (m), 1314 (w), 1285 (w), 1277 (w), 1208 (w), 1183 (m), 1162 (w), 1108 (s), 1072 (w), 1026 (w), 995 (m), 978 (w), 940 (w), 930 (w), 849 (w), 836 (w), 751 (m), 720 (s), 685 (s), 667 (m), 651 (m), 644 (m), 618 (m), 606 cm⁻¹ (m); Raman (784 nm, 50 mW, 25 °C, 4 acc., 60 s): $\tilde{\nu} = 3169$ (1), 3144 (1), 3064 (6), 3009 (1), 2992 (1), 2956 (1), 2098 (2), 2038 (1), 2024 (1), 1586 (6), 1483 (1), 1441 (1), 1353 (2), 1341 (4), 1305 (2), 1287 (1), 1231 (1), 1189 (2), 1166 (2), 1110 (2), 1100 (3), 1075 (1), 1027 (4), 1001 (10), 933 (1), 753 (1), 727 (1), 681 (2), 616 (2), 531 (1), 476 (1), 450 (1), 395 (1), 294 (2), 266 (3), 253 (3), 198 cm⁻¹ (7); elemental analysis calcd (%) for $\text{C}_{24}\text{H}_{20}\text{N}_3\text{CdP}$: C 49.88, H 3.49, N 21.81; found: C 49.48, H 3.73, N 21.68.

$[\text{PNP}]_2[\text{Cd}(\text{N}_3)_4]$

Procedure 1: To a stirred suspension of bis-bis(triphenylphosphine)iminium tetraiodo cadmate $[\text{PNP}]_2[\text{CdI}_4]$ (0.740 g, 0.44 mmol) in acetonitrile (8 mL), silver azide, AgN_3 (neat, 0.288 g, 1.92 mmol) was added in one portion at ambient temperature. The yellowish suspension was stirred for one hour and filtered (F4), resulting in a colorless solution. The solvent was removed in vacuo and the residue was dissolved in DMSO (0.6 mL). The colorless solution was allowed to evaporate over a period of two days resulting in the deposition of large colorless block-like crystals. The viscous supernatant was removed by decantation and the crystals were washed with a few drops of acetone and dried between two filter papers for five minutes. Drying in vacuo (5 mbar) over P_4O_{10} in a desiccator for 12 h gave bis-bis(triphenylphosphine)iminium tetraazido cadmate $[\text{PNP}]_2[\text{Cd}(\text{N}_3)_4]$ as colorless crystals (yield: 70–80%).

Procedure 2: Cadmium(II) azide $\text{Cd}(\text{N}_3)_2$ (0.049 g, 0.25 mmol) and bis(triphenylphosphine)iminium azide $[\text{PNP}]\text{N}_3$ (0.290 g, 0.50 mmol) were combined and dissolved in DMSO (0.6 mL) at ambient temperature. The colorless solution was allowed to evaporate over a period of two days resulting in the deposition of large colorless block-like crystals. The viscous supernatant was removed by decantation and the crystals were washed with a few drops of acetone and dried between two filter papers for five minutes. Drying in vacuo (5 mbar) over P_4O_{10} in a desiccator for 12 h gave bis-bis-(triphenylphosphine)iminium triazaazido cadmate $[\text{PNP}]_2[\text{Cd}(\text{N}_3)_4]$ as colorless crystals (yield: 70–80%). M.p. 201 °C; ^{133}Cd NMR (300 K, $[\text{D}_6]\text{DMSO}$, 111.00 MHz): $\delta = -417$ ppm ($\Delta\nu_{1/2} = 320$ Hz); ^{14}N NMR (300 K, $[\text{D}_6]\text{DMSO}$, 36.14 MHz): $\delta = -133$ (N_{br} , $\Delta\nu_{1/2} = 160$ Hz), -280 ppm (N_{tr} , $\Delta\nu_{1/2} = 830$ Hz); IR (ATR, 32 scans): $\tilde{\nu} = 3360$ (w), 3350 (w), 3081 (w), 3057 (w), 3045 (w), 3025 (w), 3012 (w), 2992 (w), 2072 (m), 2037 (s), 1586 (w), 1574 (w), 1480 (w), 1435 (m), 1313 (m), 1288 (m), 1268 (s), 1181 (w), 1157 (w), 1110 (s), 1076 (w), 1025 (w), 998 (m), 929 (w), 865 (w), 850 (w), 838 (w), 797 (w), 757 (w), 747 (m), 741 (m), 720 (s), 690 (s), 670 (m), 664 (m), 645 (w), 615 (w), 548 (s), 532 cm^{-1} (s); Raman (784 nm, 50 mW, 25 °C, 4 acc., 120 s): $\tilde{\nu} = 3172$ (1), 3147 (1), 3060 (9), 3010 (1), 2993 (1), 2956 (1), 2913 (1), 2073 (1), 2041 (1), 1589 (8), 1575 (3), 1482 (1), 1438 (1), 1338 (3), 1279 (1), 1183 (2), 1162 (2), 1111 (4), 1072 (1), 1027 (5), 1004 (10), 932 (1), 854 (1), 798 (1), 743 (1), 726 (1), 665 (3), 616 (2), 551 (1), 527 (1), 490 (1), 398 (1), 362 (1), 329 (2), 299 (1), 280 (1), 267 (2), 246 (3), 237 (3), 227 (1), 193 (2), 170 cm^{-1} (2); elemental analysis calcd (%) for $\text{C}_{72}\text{H}_{60}\text{N}_{14}\text{CdP}_4$: C 63.70, H 4.45, N 14.44; found C 63.36, H 4.53, N 14.62.

$[\text{Ph}_4\text{P}][\text{Cd}_2(\text{N}_3)_5(\text{H}_2\text{O})]$

To a stirred aqueous solution of cadmium(II) azide $\text{Cd}(\text{N}_3)_2$ (prepared by the addition of a solution of sodium azide NaN_3 (0.488 g, 7.50 mmol) in water (dist., 5 mL) to a solution of cadmium(II) sulfate $^{8/3}$ hydrate $\text{CdSO}_4^{8/3}\text{H}_2\text{O}$ (0.128 g, 0.5 mmol) in water (dist., 5 mL)), a solution of tetraphenylphosphonium chloride $[\text{Ph}_4\text{P}]\text{Cl}$ (0.124 g, 0.33 mmol) in water (dist., 3 mL) was added dropwise with rapid stirring, resulting in a colorless precipitate. The clear supernatant was removed by centrifugation and decantation and the residue was washed with water (dist., 3 mL). The supernatant was again removed by centrifugation and decantation. For recrystallization, the colorless residue was dissolved in boiling water (dist., about 15 mL) and filtered hot (F4). The resulting clear colorless solution was allowed to slowly cool to 5 °C, resulting in the precipitation of needle-like crystals. Removal of the supernatant by decantation and drying in air, followed by storage over P_4O_{10} for two days at ambient temperature (or heating to 80 °C in vacuo for about 6 h) gave tetraphenylphosphonium pentaazido dicadmium hydrate $[\text{Ph}_4\text{P}][\text{Cd}_2(\text{N}_3)_5(\text{H}_2\text{O})]$ as colorless crystals (yield: 50–60%). M.p. 266 °C; ^{133}Cd NMR (300 K, $[\text{D}_6]\text{DMSO}$, 111.00 MHz): $\delta = -540$ ($\Delta\nu_{1/2} = 310$ Hz); ^{14}N NMR (300 K, $[\text{D}_6]\text{DMSO}$, 36.14 MHz): $\delta = -132$ (N_{br} , $\Delta\nu_{1/2} = 230$ Hz), -277 (N_{tr} , $\Delta\nu_{1/2} = 1200$ Hz); IR (ATR, 32 scans): $\tilde{\nu} = 3357$ (w), 3310 (w), 3082 (w), 3063 (w), 2099 (m), 2071 (m), 2052 (m), 2024 (s), 1585 (m), 1482 (m), 1435 (m), 1327 (m), 1298 (m), 1278 (m), 1228 (m), 1185 (m), 1164 (w), 1105 (s), 1072 (w), 1027 (w), 996 (m), 942 (w), 929 (w), 921 (w), 857 (w), 847 (w), 761 (m), 754 (m), 721 (s) 687 (s), 649 (w), 636 (w), 626 (w), 619 (w), 611 (w), 604 (w), 597 cm^{-1} (w); Raman (633 nm, 2 mW, 25 °C, 8 acc., 20 s): $\tilde{\nu} = 3166$ (1), 3144 (1), 3084 (1), 3062 (3), 3047 (1), 3006 (1), 2989 (1), 2955 (1), 2134 (2), 2073 (1), 2055 (1), 2045 (1), 2032 (1), 1583 (4), 1573 (1), 1479 (1), 1433 (1), 1331 (2), 1303 (2), 1275 (1), 1228 (1), 1183 (1), 1160 (1), 1103 (1), 1093 (3), 1024 (4), 997 (10), 982 (1), 934 (1), 927 (1), 917 (1), 721 (1), 692 (1), 675 (3), 611 (2), 523 (1), 477 (1), 390 (1), 290 (1), 257 (3), 248 (4), 236 (3), 193 cm^{-1} (6); elemental

analysis calcd (%) for $\text{C}_{24}\text{H}_{22}\text{N}_{15}\text{Ocd}_2\text{P}$: C 36.38, H 2.80, N 26.52; found: C 36.41, H 2.77, N 26.49.

$[\text{Ph}_4\text{P}][\text{Hg}(\text{N}_3)_3]$

Procedure 1: To a stirred suspension of tetraphenylphosphonium triiodo mercurate $[\text{Ph}_4\text{P}][\text{HgI}_3]$ (0.276 g, 0.3 mmol) in acetonitrile (10 mL), silver azide, AgN_3 (neat, 0.148 g, 0.99 mmol) was added in one portion at ambient temperature. The colorless suspension was filtered (F4). Removal of solvent and drying in vacuo gave tetraphenylphosphonium triazido mercurate $[\text{Ph}_4\text{P}][\text{Hg}(\text{N}_3)_3]$ as a colorless microcrystalline solid (yield: 80–90%).

Procedure 2: To a stirred suspension of mercury(II) azide $\text{Hg}(\text{N}_3)_2$ (0.142 g, 0.5 mmol) in acetonitrile (5 mL), tetraphenylphosphonium azide $[\text{Ph}_4\text{P}]\text{N}_3$ (neat, 0.191 g, 0.5 mmol) was added in one portion at ambient temperature. The colorless, slightly turbid solution was filtered (F4), resulting in a colorless clear solution. Removal of solvent and drying in vacuo gave tetraphenylphosphonium triazido mercurate $[\text{Ph}_4\text{P}][\text{Hg}(\text{N}_3)_3]$ as a colorless microcrystalline solid (yield: 80–90%). M.p. 147 °C; ^{199}Hg NMR (300 K, $[\text{D}_6]\text{DMSO}$, 89.58 MHz): $\delta = -1546$ ppm ($\Delta\nu_{1/2} = 144$ Hz); ^{14}N NMR (300 K, $[\text{D}_6]\text{DMSO}$, 36.14 MHz): $\delta = -131$ (N_{br} , $\Delta\nu_{1/2} = 47$ Hz), -267 ppm (N_{tr} , $\Delta\nu_{1/2} = 428$ Hz); IR (ATR, 32 scans): $\tilde{\nu} = 3299$ (w), 3253 (w), 3055 (w), 2038 (s), 2006 (s), 1585 (w), 1483 (m), 1434 (m), 1314 (m), 1269 (m), 1183 (m), 1167 (w), 1159 (w), 1108 (s), 1074 (w), 1026 (w), 995 (m), 939 (w), 856 (w), 840 (w), 754 (m), 722 (s), 688 (s), 649 (w), 638 (w), 615 (w), 593 cm^{-1} (w); Raman (784 nm, 50 mW, 25 °C, 4 acc., 45 s): $\tilde{\nu} = 3171$ (1), 3147 (1), 3094 (2), 3066 (2), 3056 (1), 2077 (2), 2045 (1), 2008 (1), 1586 (4), 1575 (1), 1485 (1), 1442 (1), 1435 (1), 1315 (2), 1274 (1), 1266 (1), 1185 (1), 1169 (1), 1159 (1), 1109 (1), 1099 (3), 1075 (1), 1025 (10), 999 (1), 931 (1), 724 (1), 679 (3), 649 (1), 615 (3), 530 (1), 448 (1), 394 (1), 344 (6), 291 (2), 250 cm^{-1} (5); elemental analysis calcd (%) for $\text{C}_{24}\text{H}_{20}\text{N}_9\text{HgP}$: C 43.28, H 3.03, N 18.93; found: C 43.54, H 3.32, N 18.61.

$[\text{Ph}_4\text{P}]_2[\text{Hg}(\text{N}_3)_4]$

Procedure 1: To a stirred suspension of mercury(II) azide $\text{Hg}(\text{N}_3)_2$ (0.072 g, 0.25 mmol) in DMSO (1 mL), tetraphenylphosphonium azide $[\text{Ph}_4\text{P}]\text{N}_3$ (neat, 0.191 g, 0.5 mmol) was added in one portion at ambient temperature, resulting in a colorless clear solution. Slow removal of solvent and drying in vacuo gave bis-tetraphenylphosphonium tetraazido mercurate $[\text{Ph}_4\text{P}]_2[\text{Hg}(\text{N}_3)_4]$ as a colorless, crystalline solid (yield: 90–95%).

Procedure 2: To a stirred solution of tetraphenylphosphonium triazido mercurate $[\text{Ph}_4\text{P}][\text{Hg}(\text{N}_3)_3]$ (0.120 g, 0.3 mmol) in DMSO (5 mL), tetraphenylphosphonium azide $[\text{Ph}_4\text{P}]\text{N}_3$ (neat, 0.229 g, 0.6 mmol) was added in one portion at ambient temperature. The colorless solution was concentrated to an approximate volume of 3 mL in vacuo. The pale rose solution was allowed to slowly evaporate at ambient temperature in a desiccator for several hours, resulting in the deposition of colorless crystals. Removal of solvent by decantation and drying in vacuo gave bis-tetraphenylphosphonium tetraazido mercurate $[\text{Ph}_4\text{P}]_2[\text{Hg}(\text{N}_3)_4]$ as colorless crystals (yield: 80–90%).

Procedure 3 (not for preparative purposes): To a stirred colorless suspension of mercury(I) azide $\text{Hg}_2(\text{N}_3)_2$ (0.097 g, 0.2 mmol) in acetonitrile (5 mL), tetraphenylphosphonium azide $[\text{Ph}_4\text{P}]\text{N}_3$ (neat, 0.191 g, 0.5 mmol) was added in one portion at ambient temperature. The greyish suspension was stirred for one hour and filtered (F4). The colorless clear solution was concentrated to incipient crystallization in vacuo and stored at ambient temperature for ten hours. Removal of solvent by decantation and drying in vacuo

gave bis-tetraphenylphosphonium tetraazido mercurate $[\text{Ph}_4\text{P}]_2[\text{Hg}(\text{N}_3)_4]$ as colorless crystals (yield: 30–40%). M.p. 143 °C; ^{199}Hg NMR (300 K, $[\text{D}_6]\text{DMSO}$, 89.58 MHz): $\delta = -1407$ ppm ($\Delta\nu_{1/2} = 450$ Hz); ^{14}N NMR (300 K, $[\text{D}_6]\text{DMSO}$, 36.14 MHz): $\delta = -131$ (N_{br} , $\Delta\nu_{1/2} = 40$ Hz), -270 ppm (N_{tr} , $\Delta\nu_{1/2} = 300$ Hz); IR (ATR, 32 scans): $\tilde{\nu} = 3297$ (w), 3171 (w), 3079 (w), 3061 (w), 3011 (w), 2993 (w), 2049 (m), 2007 (s), 1585 (w), 1483 (m), 1435 (s), 1340 (w), 1310 (m), 1265 (m), 1188 (w), 1164 (w), 1104 (s), 1028 (m), 996 (m), 932 (w), 856 (w), 846 (w), 753 (s), 717 (s), 684 (s), 640 (m), 616 (m), 603 cm^{-1} (w); Raman (1064 nm, 500 mW, 25 °C, 500 acc.): $\tilde{\nu} = 3171$ (1), 3146 (1), 3065 (6), 3010 (1), 2993 (1), 2962 (1), 2054 (3), 2020 (1), 2010 (1), 2001 (1), 1587 (8), 1577 (3), 1485 (1), 1439 (1), 1323 (2), 1268 (1), 1191 (2), 1167 (2), 1110 (1), 1098 (2), 1029 (6), 1002 (10), 930 (1), 757 (1), 727 (1), 679 (3), 643 (1), 617 (2), 531 (1), 461 (1), 394 (1), 331 (7), 286 (2), 255 (3), 203 cm^{-1} (3); elemental analysis calcd (%) for $\text{C}_{48}\text{H}_{40}\text{N}_{12}\text{HgP}_2$: C 55.04, H 3.85, N 16.05; found: C 54.80, H 3.83, N 15.86.

[PNP][Hg(N₃)₃]

Mercury(II) azide $\text{Hg}(\text{N}_3)_2$ (0.057 g, 0.20 mmol) and bis(triphenylphosphine)iminium azide $[\text{PNP}]\text{N}_3$ (0.080 g, 0.21 mmol) were combined and dissolved in acetonitrile (2 mL) at ambient temperature. The colorless solution was allowed to evaporate in air over a period of 10 h resulting in the deposition of colorless needle-like crystals, surrounded by a solidified oil. The crystals were separated, transferred to a Schlenck tube and dried in vacuo which gave bis-(triphenylphosphine)iminium triazido mercurate $[\text{PNP}][\text{Hg}(\text{N}_3)_3]$ as colorless crystalline solid (yield: 60–70%). M.p. 119 °C; ^{199}Hg NMR (300 K, $[\text{D}_6]\text{DMSO}$, 89.58 MHz): $\delta = -1539$ ppm ($\Delta\nu_{1/2} = 640$ Hz); ^{14}N NMR (300 K, $[\text{D}_6]\text{DMSO}$, 36.14 MHz): $\delta = -131$ (N_{br} , $\Delta\nu_{1/2} = 46$ Hz), -266 ppm (N_{tr} , $\Delta\nu_{1/2} = 400$ Hz); IR (ATR, 32 scans): $\tilde{\nu} = 3309$ (w), 3279 (w), 3075 (w), 3056 (w), 3043 (w), 3025 (w), 3010 (w), 2990 (w), 2071 (m), 2041 (s), 2021 (s), 2000 (s), 1587 (w), 1481 (m), 1436 (m), 1305 (m), 1297 (m), 1232 (s), 1179 (m), 1160 (m), 1109 (s), 1027 (m), 996 (m), 981 (m), 929 (m), 893 (w), 857 (w), 847 (w), 804 (m), 759 (m), 744 (m), 720 (s), 689 (s), 666 (m), 616 (m), 606 (m), 591 (m), 532 cm^{-1} (s); Raman (784 nm, 50 mW, 25 °C, 4 acc., 60 s): $\tilde{\nu} = 3061$ (2), 2062 (1), 2036 (1), 1588 (2), 1577 (2), 1483 (1), 1440 (1), 1341 (2), 1335 (2), 1272 (1), 1181 (1), 1162 (2), 1110 (3), 1030 (4), 1002 (8), 933 (1), 850 (1), 804 (1), 850 (1), 727 (1), 667 (4), 654 (1), 615 (3), 551 (1), 525 (1), 493 (1), 449 (1), 373 (10), 282 (1), 268 (3), 249 (43), 238 (43), 229 (4), 207 cm^{-1} (3); elemental analysis calcd (%) for $\text{C}_{36}\text{H}_{30}\text{N}_{13}\text{HgP}_2$: C 49.97, H 3.49, N 16.19; found C 49.32, H 3.44, N 16.28.

[PNP]₂[Hg(N₃)₄]

Mercury(II) azide $\text{Hg}(\text{N}_3)_2$ (0.057 g, 0.20 mmol) and bis(triphenylphosphine)iminium azide $[\text{PNP}]\text{N}_3$ (0.238 g, 0.41 mmol) were combined and dissolved in acetonitrile (2 mL) at ambient temperature, resulting in a clear colorless solution. The solution was concentrated to incipient crystallization in vacuo (ca. 1 mL) and stored at ambient temperature followed by cooling at 5 °C for ten hours, resulting in the deposition of large colorless block-like crystals. The supernatant was removed by decantation and the crystals were dried in vacuo which gave bis-bis(triphenylphosphine)iminium tetraazido mercurate $[\text{PNP}]_2[\text{Hg}(\text{N}_3)_4]$ as colorless crystals. Further concentration of the mother liquor and storage at 5 °C for 20 h gave a second crop of crystals (combined yield: 80–90%). M.p. 197 °C; ^{199}Hg NMR (300 K, $[\text{D}_6]\text{DMSO}$, 89.58 MHz): $\delta = -1387$ ppm ($\Delta\nu_{1/2} = 366$ Hz); ^{14}N NMR (300 K, $[\text{D}_6]\text{DMSO}$, 36.14 MHz): $\delta = -131$ (N_{br} , $\Delta\nu_{1/2} = 40$ Hz), -270 ppm (N_{tr} , $\Delta\nu_{1/2} = 276$ Hz); IR (ATR, 32 scans): $\tilde{\nu} = 3295$ (w), 3078 (w), 3056 (w), 3045

(w), 3023 (w), 2991 (w), 2050 (w), 2007 (s), 1586 (w), 1573 (w), 1480 (w), 1433 (m), 1313 (m), 1287 (m), 1267 (s), 1180 (m), 1158 (m), 1110 (s), 1074 (m), 1025 (m), 997 (m), 929 (w), 863 (w), 851 (w), 838 (w), 798 (m), 757 (m), 746 (m), 741 (m), 720 (s), 690 (s), 664 (m), 615 (m), 548 (s), 532 cm^{-1} (s); Raman (784 nm, 0.13 mW, 25 °C, 6 acc., 15 s): $\tilde{\nu} = 3061$ (2), 2050 (1), 2026 (1), 2014 (1), 1589 (3), 1576 (1), 1483 (1), 1438 (1), 1319 (1), 1268 (1), 1181 (1), 1163 (1), 1110 (4), 1071 (1), 1028 (4), 1004 (10), 999 (2), 936 (1), 854 (1), 799 (1), 742 (1), 726 (2), 695 (1), 665 (5), 640 (1), 617 (2), 552 (1), 525 (1), 490 (1), 399 (1), 364 (1), 332 (4), 280 (1), 266 (3), 253 (2), 243 (2), 236 (4), 192 (3), 171 cm^{-1} (2); elemental analysis calcd (%) for $\text{C}_{72}\text{H}_{60}\text{N}_{14}\text{HgP}_4$: C 59.81, H 4.18, N 13.56; found: C 59.29, H 4.20, N 13.96.

[PNP][Hg(N₃)₂(CH₃CN₄)]

The mother liquor from crystallization of $[\text{PNP}]_2[\text{Hg}(\text{N}_3)_4]$ (obtained by the reaction of mercury(II) azide and $[\text{PNP}]\text{N}_3$ in acetonitrile) was concentrated in vacuo and stored for two days at 5 °C, resulting in the deposition of needle-like crystals. The crystalline residue was warmed to ambient temperature to partly dissolve the solid. The supernatant was removed by decantation and the crystals were dried in vacuo which gave bis(triphenylphosphine)iminium diazido(5-methyl-1H-tetrazol-1-yl)mercurate acetonitrile hemisolvate $[\text{PNP}][\text{Hg}(\text{N}_3)_2(\text{CH}_3\text{CN}_4)] \cdot 0.5\text{CH}_3\text{CN}$ as colorless crystals. Solvent-free crystals of $[\text{PNP}][\text{Hg}(\text{N}_3)_2(\text{CH}_3\text{CN}_4)]$ were obtained by recrystallization from DMSO at ambient temperature. Yields were not determined.

[PNP][Hg(N₃)₂(CH₃CN₄)] · 0.5 CH₃CN: M.p. 122 °C (66 °C loss of CH_3CN); ^{199}Hg NMR (300 K, $[\text{D}_6]\text{DMSO}$, 89.58 MHz): $\delta = -1420$ ppm ($\Delta\nu_{1/2} = 1380$ Hz); ^1H - ^{15}N -HMBC (300 K, $[\text{D}_6]\text{DMSO}$, 500.13, 50.69 MHz): $\delta = -80$ ($\text{CH}_3\text{CN}_2\text{N}_2$), 8.3 ppm ($\text{CH}_3\text{CN}_2\text{N}_2$); ^{14}N NMR (300 K, $[\text{D}_6]\text{DMSO}$, 36.14 MHz): $\delta = -131$ (N_{br} , $\Delta\nu_{1/2} = 51$ Hz), -267 ppm (N_{tr} , $\Delta\nu_{1/2} = 380$ Hz); ^{13}C NMR (300 K, $[\text{D}_6]\text{DMSO}$, 125.8 MHz): $\delta = 1.08$ (s, CH_3CN), 9.52 (s, CH_3CN_4), 118.0 (s, CH_3CN), 126.8 (dd, $^1J(^{13}\text{C}-^{31}\text{P}) = 107.2$ Hz, $^3J(^{13}\text{C}-^{31}\text{P}) = 1.71$ Hz, *ipso*-Ph), 129.5 (m, *meta*-Ph), 131.9 (m, *ortho*-Ph), 133.6 (s, *para*-Ph), 156.9 ppm (s, CH_3CN_4); ^1H NMR (300 K, $[\text{D}_6]\text{DMSO}$, 500.13 MHz): $\delta = 2.07$ (s, 1.5H, CH_3CN , $^1J(^{13}\text{C}-^1\text{H}) = 136$ Hz), 2.38 (s, 3H, CH_3CN_4), 7.52–7.65 (m, 24H, *ortho/meta*-Ph), 7.70 ppm (m, 6H, *para*); IR (ATR, 32 scans): $\tilde{\nu} = 3307$ (w), 3090 (w), 3078 (w), 3057 (w), 3025 (w), 2992 (w), 2934 (w), 2286 (w), 2253 (w), 2022 (s), 1588 (m), 1574 (w), 1495 (w), 1482 (m), 1435 (s), 1378 (m), 1285 (s), 1251 (s), 1181 (m), 1159 (m), 1110 (s), 1070 (m), 1025 (m), 997 (m), 927 (w), 854 (w), 845 (w), 803 (m), 761 (m), 745 (m), 720 (s), 689 (s), 665 (m), 616 (w), 546 (s), 530 cm^{-1} (s); Raman (784 nm, 21 mW, 25 °C, 4 acc., 75 s): $\tilde{\nu} = 3178$ (1), 3148 (1), 3064 (3), 3013 (1), 2995 (1), 2937 (1), 2258 (1), 2252 (1), 2052 (1), 2046 (1), 1590 (4), 1577 (2), 1498 (1), 1487 (1), 1441 (1), 1391 (1), 1376 (1), 1326 (1), 1274 (1), 1253 (1), 1241 (1), 1183 (1), 1162 (1), 1112 (4), 1072 (1), 1029 (5), 1003 (10), 928 (1), 848 (1), 804 (1), 761 (1), 748 (1), 725 (1), 700 (1), 691 (21), 665 (5), 648 (1), 617 (5), 552 (1), 527 (1), 495 (1), 439 (1), 402 (1), 370 (1), 331 (5), 283 (1), 270 (2), 249 (4), 239 cm^{-1} (4); elemental analysis calcd (%) for $\text{C}_{39}\text{H}_{34.5}\text{N}_{11.5}\text{HgP}_2$: C 50.54, H 3.75, N 17.38; found C 50.07, H 3.90, N 17.61.

[PNP]₂[Hg(N₃)₂(CH₃CN₄)]: M.p. 122 °C; IR (ATR, 32 scans): $\tilde{\nu} = 3295$ (w), 3093 (w), 3077 (w), 3058 (w), 3025 (w), 2992 (w), 2936 (w), 2059 (m), 2038 (s), 2026 (s), 1587 (w), 1574 (w), 1481 (m), 1435 (s), 1363 (m), 1307 (m), 1274 (m), 1244 (s), 1181 (m), 1162 (m), 1108 (s), 1065 (m), 1025 (m), 997 (m), 929 (w), 853 (w), 845 (w), 802 (m), 758 (m), 746 (m), 719 (s), 689 (s), 666 (m), 616 (w), 551 cm^{-1} (s); Raman (633 nm, 5 mW, 25 °C, 5 acc., 20 s): $\tilde{\nu} = 3174$ (1), 3148 (1), 3065 (6), 3027 (1), 3010 (1), 2993 (1), 2957 (1), 2940 (1), 2062 (1), 2042 (1),

2030 (1), 1588 (4), 1576 (1), 1492 (1), 1449 (1), 1441 (1), 1388 (1), 1322 (1), 1278 (1), 1243 (1), 1185 (1), 1166 (1), 1111 (3), 1067 (1), 1030 (5), 1002 (10), 945 (1), 927 (1), 855 (1), 845 (1), 804 (1), 790 (1), 746 (1), 724 (1), 692 (2), 668 (3), 661 (2), 618 (2), 554 (1), 527 (1), 496 (1), 385 (1), 371 (1), 351 (5), 319 (1), 281 (1), 251 (4), 238 cm⁻¹ (4).

Acknowledgements

Dipl. Chem. Alexander Hinz (University Rostock), Dipl. Chem. Fabian Reiß (University Rostock), and M.Sc. Kati Rosenstengel (University Rostock) are acknowledged for helpful advice. Dr. Dirk Michalik (University Rostock) is acknowledged for NMR measurements. We thank the DFG (grant SCHU 1170 8-1), the University of Rostock, and the Leibniz Institute for Catalysis for financial support.

Keywords: azides · cadmium · cycloaddition · mercury · structure elucidation

- [1] a) I. C. Tornieporth-Oetting, T. M. Klapötke, *Angew. Chem. Int. Ed. Engl.* **1995**, *34*, 511–520; *Angew. Chem.* **1995**, *107*, 559–568; b) W. P. Fehlhammer, W. Beck, *Z. Anorg. Allg. Chem.* **2013**, *639*, 1053–1082.
- [2] a) T. Curtius, *Chem. Ber.* **1890**, *23*, 3023–3033; b) M. Berthelot, P. Vieille, *Bull. Soc. Chim. Paris* **1894**, *11*, 744–748.
- [3] a) D. Seybold, K. Dehnicke, *Z. Anorg. Allg. Chem.* **1968**, *361*, 277–283; b) P. Nockemann, U. Cremer, U. Ruschewitz, G. Meyer, *Z. Anorg. Allg. Chem.* **2003**, *629*, 2079–2082; c) B. L. Evans, A. D. Yoffe, P. Gray, *Chem. Rev.* **1959**, *59*, 515–566; d) L. Wöhler, W. Krupko, *Chem. Ber.* **1913**, *46*, 2045–2057; e) L. Wöhler, F. Martin, *Angew. Chem.* **1917**, *30*, 33–39.
- [4] a) T. R. Musgrave, R. N. Keller, *Inorg. Chem.* **1965**, *4*, 1793–1796; b) U. Müller, *Z. Anorg. Allg. Chem.* **1973**, *399*, 183–192; c) F. D. Miles, *J. Chem. Soc.* **1931**, 2532–2542.
- [5] H. Lund, O. Oeckler, T. Schröder, A. Schulz, A. Villinger, *Angew. Chem. Int. Ed.* **2013**, *52*, 10900–10904.
- [6] W. Strecker, E. Schwinn, *J. Prakt. Chem.* **1939**, *152*, 205–218.
- [7] a) A. Perret, R. Perrot, *Helv. Chim. Acta* **1933**, *16*, 848–857; b) K. Dehnicke, J. Strähle, D. Seybold, J. Müller, *J. Organomet. Chem.* **1966**, *6*, 298–300; c) K. Dehnicke, D. Seybold, *J. Organomet. Chem.* **1968**, *11*, 227–241; d) A. F. Shihada, K. Dehnicke, *J. Organomet. Chem.* **1971**, *26*, 157–160; e) D. J. Brauer, H. Bürger, G. Pawelke, K. H. Flegler, A. Haas, *J. Organomet. Chem.* **1978**, *160*, 389–401; f) T. M. Klapötke, B. Krumm, R. Moll, *Z. Anorg. Allg. Chem.* **2011**, *637*, 507–514; g) T. M. Klapötke, B. Krumm, R. Moll, *Eur. J. Inorg. Chem.* **2011**, 422–428.
- [8] W. Beck, W. P. Fehlhammer, P. Pöllmann, E. Schuierer, K. Feldl, *Chem. Ber.* **1967**, *100*, 2335–2361.
- [9] a) T. Curtius, J. Rissom, *J. Prakt. Chem.* **1898**, *58*, 261–309; b) L. Birckenbach, *Z. Anorg. Allg. Chem.* **1933**, *214*, 94–96.
- [10] a) F. P. Bowden, K. Singh, *Proc. R. Soc. London Ser. A* **1954**, *227*, 22–37; b) F. Karau, W. Schnick, *Z. Anorg. Allg. Chem.* **2005**, *631*, 2315–2320.
- [11] a) M. Bassière, *Compt. Rend.* **1937**, *204*, 1573–1574; b) O. Reckeweg, A. Simon, *Z. Naturforsch. B* **2003**, *58*, 1097–1104.
- [12] a) I. Agrell, *Acta. Chem. Scand.* **1970**, *24*, 3575–3589; b) N. Mondal, M. K. Saha, S. Mitra, V. Gramlich, *J. Chem. Soc. Dalton Trans.* **2000**, 3218–3221; c) M. A. S. Goher, F. A. Mautner, M. A. M. Abu-Youssef, A. K. Hafez, A. M.-A. Badr, *J. Chem. Soc. Dalton Trans.* **2002**, 3309–3312; d) M. A. S. Goher, F. A. Mautner, A. K. Hafez, M. A. M. Abu-Youssef, C. Gspan, A. M.-A. Badr, *Polyhedron* **2003**, *22*, 975–979; e) F. A. Mautner, C. Gspan, M. A. S. Goher, M. A. M. Abu-Youssef, *Monatsh. Chem.* **2005**, *136*, 107–117; f) A. Kriza, M. Tatucu, *J. Coord. Chem.* **2011**, *64*, 195–201.
- [13] a) W. Clegg, H. Krischner, A. I. Saracoglu, G. M. Sheldrick, *Z. Kristallogr.* **1982**, *161*, 307–313; b) H. Haselmair, H. Krischner, *Z. Anorg. Allg. Chem.* **1980**, *468*, 76–77.
- [14] a) S. Hanna, F. A. Mautner, B. Koppelhuber-Bitschnau, M. A. M. Abu-Youssef, *Mater. Sci. Forum* **2000**, *321–324*, 1098–1101; b) Z.-Y. Du, Y.-P. Zhao, W.-X. Zhang, H.-L. Zhou, C.-T. He, W. Xue, B.-Y. Wang, X.-M. Chen, *Chem. Commun.* **2014**, *50*, 1989–1991.
- [15] H. Krischner, C. Kratky, H. E. Maier, *Z. Kristallogr.* **1982**, *161*, 225–229.
- [16] Full set of experimental data for all considered Cd and Hg azides can be found in the Supporting Information. Synthesis and full characterization of all starting materials including X-ray structure elucidation of [PNP][Cd₃], [PNP]₂[Cd₄], [Ph₄P][Hg₃] and [Ph₄P]₂[Hg₄].CH₂Cl₂.
- [17] D. W. M. Hofmann, *Acta Crystallogr. B* **2002**, *58*, 489–493.
- [18] a) B. Neumüller, F. Schmock, S. Schlecht, K. Dehnicke, *Z. Anorg. Allg. Chem.* **2000**, *626*, 1792–1796; b) R. Haiges, A. Vij, J. A. Boatz, S. Schneider, T. Schroer, M. Gerken, K. O. Christe, *Chem. Eur. J.* **2004**, *10*, 508–517; c) K. Rosenstengel, A. Schulz, A. Villinger, *Inorg. Chem.* **2013**, *52*, 6110–6126.
- [19] A. Villinger, A. Schulz, *Angew. Chem. Int. Ed.* **2010**, *49*, 8017–8020; *Angew. Chem.* **2010**, *122*, 8190–8194.
- [20] a) R. S. Berry, *J. Chem. Phys.* **1960**, *32*, 933–940; b) M. Sandström, I. Persson, S. Ahrlund, *Acta. Chem. Scand. A* **1978**, *32*, 607–625.
- [21] a) J. D. Kennedy, W. McFarlane, *J. Chem. Soc. Perkin Trans. 2* **1977**, 1187–1191; b) R. J. Kostelnik, A. A. Bothner-By, *J. Magn. Reson. (1969–1992)* **1974**, *14*, 141–151; c) M. A. Sens, N. K. Wilson, P. D. Ellis, J. D. Odom, *J. Magn. Reson. (1969–1992)* **1975**, *19*, 323–336.
- [22] G. Klose, F. Volke, G. Peinel, G. Knobloch, *Magn. Reson. Chem.* **1993**, *31*, 548–551.
- [23] Holleman Wiberg, *Lehrbuch der Anorganischen Chemie*, 102. Aufl., Walter de Gruyter, Berlin, **2007**, Anhang IV.
- [24] F. A. Mautner, H. Krischner, C. Kratky, *Z. Kristallogr.* **1985**, *172*, 291–296.
- [25] P. Pyykkö, M. Atsumi, *Chem. Eur. J.* **2009**, *15*, 12770–12779.
- [26] J. E. Carpenter, F. Weinhold, *J. Mol. Struct.* **1988**, *169*, 41–62.
- [27] F. Weinhold, J. E. Carpenter, *The Structure of Small Molecules and Ions*, **1988**, Plenum, pp. 227–236.
- [28] F. Weinhold, C. Landis, *Valency and Bonding: A Natural Bond Orbital Donor–Acceptor Perspective*, **2005**, Cambridge University Press, and references therein.
- [29] D. Figgen, G. Rauhut, M. Dolg, H. Stoll, *Chem. Phys.* **2005**, *311*, 227–244.
- [30] K. A. Peterson, C. Puzarini, *Theor. Chem. Acc.* **2005**, *114*, 283–296.

Received: November 8, 2014

Published online on January 22, 2015